PALEOCEANOGRAPHY, VOL. 6, NO. 1, PAGES 33-52, FEBRUARY 1991

MIOCENE ISOTOPE REFERENCE SECTION, DEEP SEA DRILLING PROJECT SITE 608: AN EVALUATION OF ISOTOPE AND BIOSTRATIGRAPHIC RESOLUTION

Kenneth G. Miller[1] and Mark D. Feigenson

Department of Geological Sciences,
Rutgers University, New Brunswick, New Jersey

James D. Wright

Lamont-Doherty Geological Observatory
and Department of Geological Sciences,
Columbia University, Palisades, New York

Bradford M. Clement

Department of Geology
Florida International University, Miami

Abstract. We developed an isotope ($^{87}Sr/^{86}Sr$, $\delta^{18}O$) reference section for the uppermost Oligocene to lower upper Miocene (ca. 25-8 Ma) at Site 608 in the northeastern North Atlantic. This site contains the least ambiguous magnetostratigraphic record of Miocene polarity changes available, providing direct correlations to the Geomagnetic Polarity Time Scale (GPTS). We integrate biostratigraphic, magnetostratigraphic, Sr isotope, and stable isotope data to provide a reference section for Miocene isotope fluctuations. The direct correlation of isotopes and biostratigraphy to the Geomagnetic Polarity Time Scale (GPTS) provides relatively precise age estimates. We use these age estimates to evaluate the timing of first and last occurrences of planktonic foraminifera, and conclude that many of these are synchronous within a 0.5 m.y. resolution between subtropical Site 563 (33°N) and high-latitude Site 608 (43°N). In addition, we use this chronology to estimate the ages of previously established Miocene oxygen isotope Zones Mi1 through Mi7 and to compare the Sr isotope record at Site 608 with previously published $^{87}Sr/^{86}Sr$ records. We approximate latest Oligocene to early late Miocene (25-8 Ma) Sr isotope changes with two linear regressions. The rate of increase of $^{87}Sr/^{86}Sr$ was high from the latest Oligocene (~25 Ma) to earliest middle Miocene (~15 Ma), with an estimated rate of 0.000059/m.y. Our ability to reproduce Sr isotope measurements is ±0.000030 or better, yielding a stratigraphic resolution of as good as ±0.5 m.y. for this interval. The rate of change was much lower from about 15 to 8 Ma (on average, 0.000013/m.y.), yielding Sr isotope stratigraphic resolution of worse than ±2.3 m.y. The causes of the late Eocene to Miocene $^{87}Sr/^{86}Sr$ increases are not known. We speculate that a moderate $^{87}Sr/^{86}Sr$ increase (0.000030/m.y) which occurred during the late Eocene-latest Oligocene can be explained by intermittent glaciations and deglaciations of the Antarctic continent. These pulse-like changes in the input of glacial weathering products yield what appears to be a monotonic, linear increase. The increase in the frequency of glaciations during the latest Oligocene-early Miocene can explain the higher rate of change of $^{87}Sr/^{86}Sr$ at this time. We speculate that by the middle Miocene, the development of a permanent east Antarctica ice sheet resulted in decreased input of glacial weathering products and a lower rate of $^{87}Sr/^{86}Sr$ change.

BACKGROUND

Firm stratigraphic correlations are indispensable for solving problems in earth history. Stratigraphic correlations of Cenozoic marine strata have improved considerably during the past 35 years as a result of four advances:

1. Development of relatively refined planktonic zonations allowed correlation of pelagic sediments with a 0.5-4.0 m.y. resolution (e.g., Bolli [1957]; Blow [1969, 1979]; Martini [1971]; see discussions of Bolli et al. [1985], Miller and Kent [1987], and Berggren and Miller [1988]).
2. Recovery of relatively continuous deep-sea sections by the Deep Sea Drilling Project (DSDP) and Ocean Drilling Program (ODP) provided requisite material for improving stratigraphic correlations.
3. Examination of deep-sea sections exposed on land and from DSDP/ODP sites revealed polarity changes which can be correlated with the GPTS [e.g., Lowrie et al., 1982; Tauxe et al., 1983, 1984].
4. Beginning with Shackleton and Kennett [1975] and Savin et al. [1975], oxygen and carbon isotope measurements of pre-Pleistocene deep-sea sections led to the development of isotope stratigraphy for this interval.

[1]Also at Lamont-Doherty Geological Observatory of Columbia University, Palisades, New York

Paper number 90PA01941.
0883-8305/91/90PA-01941$10.00.

Each of these advances led to improvements in our ability to discriminate finer time intervals for the Cenozoic. More significantly, the integration of biostratigraphy, magnetostratigraphy, and isotope stratigraphy provided greatly improved correlations [Berggren et al., 1985; Miller et al., 1985; Miller and Kent, 1987]. Nevertheless, uncertainties in these methods are not fully appreciated, and estimates of stratigraphic resolution are often exaggerated (discussion of Miller and Kent [1987]).

The pioneering work of Burke et al. [1982] showed that $^{87}Sr/^{86}Sr$ changes in marine carbonates could be used for Phanerozoic correlations. The Sr isotope correlation method is not a radioisotope age measurement; rather, it relies on matching Sr isotope measurements for "unknowns" to an empirical calibration of seawater $^{87}Sr/^{86}Sr$ changes. The Sr isotope ratio in seawater is believed to be uniform at any given time, since the residence time is much longer than oceanic mixing times [Broecker and Peng, 1982]. A large increase in the $^{87}Sr/^{86}Sr$ record occurred from the late Eocene to Recent [Burke et al., 1982]. Because of this change, the Sr isotope stratigraphy of this interval offers the potential for unique stratigraphic correlations.

Sr isotope stratigraphy is particularly useful in regions where conventional stratigraphic techniques sometimes fail. Sr isotope stratigraphy allows the correlation of high-latitude and shallow water (neritic) sections to standard low-latitude chronologies (for example, see Rundberg and Smalley [1989], McNeil and Miller [1990], and Miller et al. [1990b]). Such deposits can be difficult to correlate because of the absence of diagnostic marker fossils and the general unsuitability of shallow water deposits for magnetostratigraphic studies.

Sr isotope stratigraphy requires unequivocal age calibrations of seawater $^{87}Sr/^{86}Sr$ variations recorded in carbonates. Changes in Cenozoic $^{87}Sr/^{86}Sr$ values have been delineated in several laboratories since Burke et al. [1982](overall Tertiary: DePaolo and Ingram [1985], Hess et al. [1986], and Koepnick et al. [1985, 1988]; late Eocene-Oligocene: Miller et al. [1988] and Hess et al. [1989]; Miocene-Recent: DePaolo [1986], McKenzie et al. [1988], Hodell et al. [1989, 1990a,b], and Capo and DePaolo [1990]) These studies have relied on biostratigraphy or magnetostratigraphy to obtain their age calibrations.

The initial attempts to calibrate Sr isotopes versus age relied on biostratigraphy [Burke et al., 1982; DePaolo and Ingram, 1985; DePaolo 1986; Hess et al., 1986; Koepnick et al., 1985, 1988]. However, there are inherent errors of 0.5-4.0 m.y. in biostratigraphic age estimates [Miller and Kent, 1987]. Biostratigraphic correlations are often complicated by varying taxonomic and stratigraphic interpretations and by diachronous and geographically restricted ranges [Miller et al., 1985, 1988; Miller and Kent, 1987; Hess et al., 1989]. Only in rare instances can biostratigraphic correlations provide resolution better than 0.5 m.y. Therefore, correlations of isotope records based on biostratigraphy require independent verification.

Subsequent studies correlated directly to the GPTS by measuring isotope fluctuations in sections with unambiguous magnetostratigraphy [Miller et al., 1988; McKenzie et al., 1988; Hodell et al., 1989, 1990a,b; Hess et al., 1989]. Two different philosophies exist in constructing a Sr isotope standard using first-order calibrations. One relies on measuring isotope fluctuations in more than one section and "stacking" the results [McKenzie et al., 1988; Hess et al., 1989; Hodell et al., 1989, 1990a,b]. Stacking fills in gaps that may be present in a given section and removes random noise by cancellation. However, stacking records potentially suffers from biostratigraphic problems because the errors in biostratigraphy are not random. This is not a problem if all of the sections have excellent magnetostratigraphy. However, coring gaps, intervals of uncertain polarity, and unconformities complicate magnetostratigraphic interpretations. There is no Cenozoic series which has an unambiguous magnetostratigraphy at one location, let alone more than one section. By using more than one section, these studies ultimately rely on biostratigraphy for correlation. In fact, these studies have employed sections with no magnetostratigraphy in their composite standards, relying on biostratigraphic age estimates in making the composites.

Our approach has been to develop individual isotope reference sections for the Oligocene (Site 522 [Miller et al., 1988]) and the lower to lower upper Miocene (Site 608; this study). These sections contain the most complete, least complicated magnetostratigraphic records available for these intervals [Tauxe et al., 1983, 1984; Clement and Robinson, 1986] and provide a time rock reference for the timing of isotope fluctuations (see discussion section).

Stable isotope stratigraphy differs from Sr isotope correlations. Oxygen and carbon isotope correlations rely on matching patterns of change and therefore are usually not unique. Oxygen isotope stratigraphy has become the standard Quaternary correlation tool, where astronomical changes ("Milankovitch" periodicity; ~100 kyr, 41 kyr, and 23 kyr) provide a resolution of approximately 5 kyr [Imbrie et al., 1984]. The possibility of extending this high-resolution stratigraphy into the late Pliocene was suggested by Ruddiman et al. [1986a], Raymo et al. [1989], and Joyce et al. [1990]. Similar high-frequency $\delta^{18}O$ fluctuations have been suggested for the middle and late Miocene [Pisias et al., 1985; Keigwin et al., 1986]. It has proven difficult to develop a high-resolution (10^4-10^5 yr) $\delta^{18}O$ time scale for the pre-Pliocene because of problems in sampling resolution and stratigraphic correlations. Although "Milankovitch" resolution has not been developed for the pre-Pliocene, studies show that stable isotopes can be used to improve Cenozoic correlations on the m.y. scale [e.g., Haq et al., 1980; Miller et al., 1989, 1990a]. We previously identified 12 $\delta^{18}O$ increases which occurred during the Oligocene to early late Miocene (between ~36 and 8 Ma) and used them to recognize formally oxygen isotope zones Oi1-Oi3 and Mi1-Mi7 [Miller et al., 1990a; Wright and Miller, 1990]. Many of these zones have been defined at Site 608; the magnetostratigraphy presented here is used to correlate these isotope zones to the GPTS and to derive their age estimates. We used these oxygen isotope events and zones to improve high-latitude stratigraphic correlations to the GPTS [Wright and Miller, 1990].

Calibration of the first occurrences (FO) and last occurrences (LO) of planktonic foraminifera against magnetostratigraphy documents that some low-latitude taxa exhibit latitudinal diachrony [Miller et al., 1985; Weaver and Clement, 1986; Dowsett, 1988; Hess et al., 1989]. Low-latitude biozones are difficult to apply at high latitudes for this reason [e.g., Jenkins, 1985]. Certain Plio-Pleistocene planktonic foraminifera had diachronous first and last occurrences [Weaver and Clement, 1986; Dowsett, 1988]. Miller et al. [1985] documented that many Oligocene-Miocene tropical planktonic foraminiferal zones are applicable at subtropical Sites 563 (33°N) and 558 (38°N), although they interpreted the absence or juxtaposition of some zonal markers to reflect diachronous ranges. For example, the zonal criteria for Miocene Zones N4a, N4b, N5, N7, N8, N11, and N12 are present in the proper biochronologic sequence at Sites 563 and

558, but the markers for Zones N14 (FO of *Globigerina nepenthes*) and N16 (FO of *Neogloboquadrina acostaensis*) are juxtaposed with those for Zones N13 (LO *Globorotalia fohsi* spp.) and N15 (LO *Globorotalia mayeri*), respectively. Miller et al. [1985] interpreted the resulting absence of tropical Zones N13 and N15 to reflect diachronous first and last occurrences rather than hiatuses. This supposition needs to be tested against magnetostratigraphy at other locations. Site 608 may provide this opportunity since it lies at a critical latitude (43°) for evaluating the applicability of tropical zones and synchrony and diachrony of planktonic marker species at higher latitudes.

The Miocene is a particularly interesting interval for developing improved isotope stratigraphic control. The modern oceans began to evolve during the Miocene epoch [Kennett, 1977, 1985; Wright et al., 1990; etc.], and there were numerous inferred global sea level changes during this interval [Haq et al., 1987]. Although middle Miocene biozonations are relatively precise, early Miocene biostratigraphic control is often poor because of long biozones and the absence of marker taxa in certain intervals. There was a high rate of $^{87}Sr/^{86}Sr$ increase during the early to early middle Miocene [DePaolo and Ingram, 1985; Hess et al., 1986], and there were several global oxygen and carbon isotope fluctuations. Therefore isotopes can provide improved correlations for this interval. DSDP Site 608 (eastern North Atlantic; 42°50.20'N, 23°05.25'W; 3526 m present water depth; ~3100-3500 m Miocene water depth [Miller et al., 1986]) provides an excellent Miocene magnetostratigraphic record [Clement and Robinson, 1986; this study]. We chose to focus on this section rather than on other sections with published magnetostratigraphy (e.g., Site 516 [Berggren et al. 1983a,b, Hess et al. 1989]) because of its superior magnetostratigraphic record. Initial oxygen and carbon isotope analyses of the Site 608 Miocene section have demonstrated its suitability for isotope analyses [Miller et al., 1986; Miller et al., 1990a; Wright et al., 1990]. We analyzed the $^{87}Sr/^{86}Sr$ and $\delta^{18}O$ composition of foraminiferal tests from this section (carbon isotope results will be presented by Wright et al. [1990 and manuscript in preparation, 1990]). We supplemented the magnetostratigraphic measurements of Clement and Robinson [1986] and evaluated planktonic foraminiferal biostratigraphy. This establishes first-order calibrations of the isotope and biostratigraphic records with the GPTS.

METHODS

Magnetostratigraphy

Site 608 provides the most complete sedimentary documentation of early to early late Miocene (ca. 23-8 Ma) geomagnetic polarity changes [Clement and Robinson, 1986]. Still, there are some levels at Site 608 with ambiguous correlations to the GPTS within this interval of frequent reversals. We resampled the section between Cores 25 and 41 (387-224 meters subbottom (msb)) for paleomagnetic study to refine the placement of reversal boundaries and to define short polarity intervals. An additional 60 samples were obtained bringing the paleomagnetic sampling interval to two or three samples per section (1.5 m). Each additional sample was subjected to partial alternating field demagnetization at peak fields of 15-25 mT and measured using a three axis cryogenic magnetometer at Florida International University. The resulting inclination data were combined with that of Clement and Robinson [1986] to provide our best estimate of polarity reversals recorded at Site 608 (Figure 1). The declination, inclination, and intensity data for all samples are included in Appendix 1[1]. The GPTS of Berggren et al. [1985] was used in making all age estimates (Table 1) and in drawing all boundaries.

Based on stable isotope correlations [Wright and Miller, 1990] and biostratigraphy [Takayama and Sato, 1986; this study], we made minor changes in the identification of the magnetochronozones at Site 608 (Figure 1). The Oligocene/Miocene boundary at Site 608 is between Samples 42-2, 38-40 cm (417.58 msb) and 45-2, 44-45 cm (417.64 msb), because *Turborotalia* cf. *kugleri* first occurs in the former sample (Figure 1) and *Reticulofenestra bisecta* last occurs in the latter sample [Takayama and Sato, 1986]. These biostratigraphic events have been correlated elsewhere with the base of Chron C6Cn2 and the Oligocene/Miocene boundary [e.g., Berggren et al., 1985]. Thus, we suggest that the three normal polarity intervals of Chron C6C are not represented at Site 608, Chronozone C6n2 is concatenated with C6Cn3 (Figure 1), and the base of C6Cn lies at 419.74 msb (Table 1). Stable isotope correlations also suggest this interpretation (see below).

The polarity pattern below 420 msb (Figure 1) cannot be correlated to the GPTS in a straightforward manner. One interpretation would identify a normal magnetozone between 428 and 425 msb as Chronozone C7n. However, the LO of definite *Sphenolithus ciperoensis* is in Sample 46-2, 46-47 cm (427.26 msb)[Takayama and Sato, 1986]; this taxon last occurs in the suspect normal at Site 608, but last occurs above Chronozone C7n elsewhere (25.2 Ma)[Berggren et al., 1985]. In addition, the identification of Chronozone C7n requires greatly reduced sedimentation rates for C6Cr. To obtain age estimates for this section, we extrapolated sedimentation rates from the base of Chronozone C6cn (Table 1). Our age estimates for Core 26 are consistent with the biostratigraphic data, although we caution that age estimates for this interval are not certain.

A normal magnetozone between 391 and 402 msb was previously interpreted as Chronozone C6A [Clement and Robinson, 1986; Miller et al., 1988]. Our correlation of the underlying normal magnetozone to C6Cn suggests that the overlying zone is C6Bn, not C6An as previously believed. Our stable isotope correlations with Sites 563 and 747 also indicate that the interval between 391 and 402 msb is Chronozone C6Bn (Wright and Miller, [1990]; see below). Chronozones C6A and C6 appear to be concatenated; isotope correlations suggest that most of Chronozone C5En is present (Wright and Miller, [1990]; see below) which is consistent with the revised polarity interpretation (Figure 1). Still, there may be an unconformity in the lower Miocene section between 364 and 382 msb. In the age model used here, the interval from 390 to 375 msb has a mean sedimentation rate of only 7 m/m.y. (Table 1, age model 1). We present an alternate age model in which Chron C6A is not represented at Site 608 (~1 m.y. hiatus; Table 1, age model 2). The differences between the age models do not affect the Sr isotope regressions discussed below.

Site 608 magnetozones match the GPTS between Cores 39 and 20, although some shorter polarity changes are not

---

[1] Appendix 1 is available with entire article on microfiche. Order from American Geophysical Union, 2000 Florida Avenue N.W., Washington, D.C. 20009. Document P90-001;$2.50. Payment must accompany order.

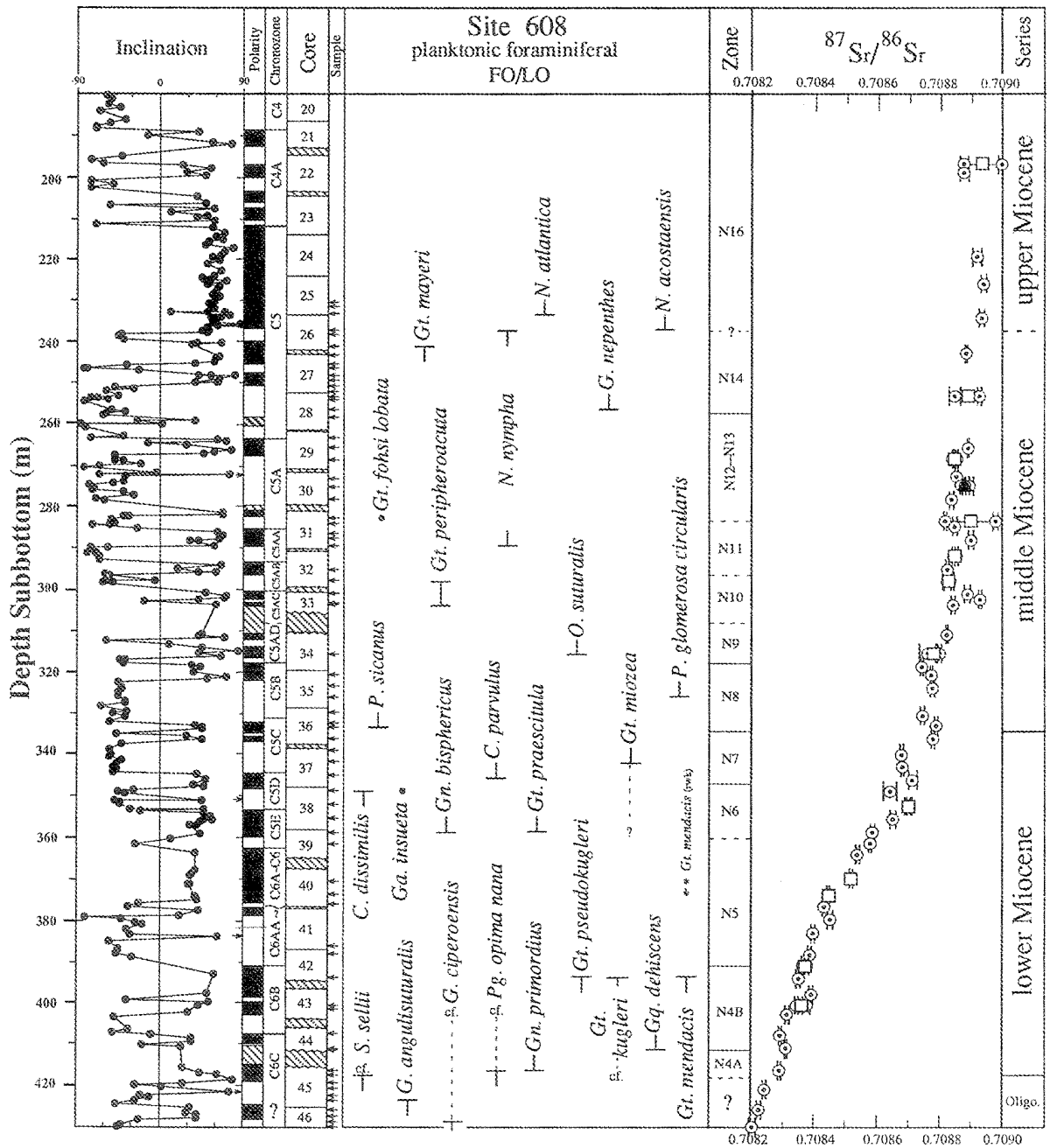

Fig. 1. Uppermost Oligocene to lower middle Miocene magnetostratigraphy, planktonic foraminiferal biostratigraphy, and Sr isotope stratigraphy, eastern North Atlantic DSDP Site 608. Inclination data after Clement and Robinson [1986] and this study; positive or negative inclinations indicate normal (shaded) or reversed (open) magnetic polarities. Magnetochronostratigraphic interpretation is that of Wright and Miller [1990] and this study. Single polarity excursions are indicated with arrows. Slashes in polarity column indicate uncertain polarities; slashes in core column indicate intervals with no recovery. Tick marks indicate samples examined for biostratigraphy. Circles indicate single occurrences, asterisks indicate occurrences interpreted as reworked, and dashed lines indicate uncertain range. Sr isotope analyses are indicated with open circles with small solid circles. Error bars are analytical precision (Table 2). Squares indicate the mean of duplicate analyses, while the triangle indicates the mean of a triplicate analysis.

TABLE 1. Age Model Parameters, Site 608

Depth, msb	Age, Ma	Sedimentation Rate, m/m.y.	Criterion
Age model 1, Assumes Condensed Interval in Chronozones C6n-C6A			
179.32	7.41		base of Chronozone C4
188.87	7.90	19.49	top of Chronozone C4A
211.87	8.92	22.55	top of Chronozone C5
263.70	11.55	19.71	top of Chronozone C5A
285.62	12.83	17.13	top of Chronozone C5AA
293.62	13.20	21.62	top of Chronozone C5AB
299.71	13.69	12.43	top of Chronozone C5A
322.43	15.27	14.38	base of Chronozone C5B
332.49	16.22	10.59	top of Chronozone C5
344.68	17.57	9.03	top of Chronozone C5D
353.94	18.56	9.35	top of Chronozone C5E
362.73	19.35	11.13	top of Chronozone C6
375.39	20.45	11.51	base of Chronozone C6n
390.62	22.57	7.18	top of Chronozone C6B
408.23	23.27	25.16	top of Chronozone C6n3
419.74	24.21	12.25	base of Chronozone C6n1
			extrapolate to 430.01 msb
Age Model 2, Assumes Unconformity Chronozone C6A			
179.32	7.41	20.39	base of Chronozone C4
188.87	7.90	19.49	top of Chronozone C4A
211.87	8.92	22.55	top of Chronozone C5
263.70	11.55	19.71	top of Chronozone C5A
285.62	12.83	17.13	top of Chronozone C5AA
293.62	13.20	21.62	top of Chronozone C5AB
299.71	13.69	12.43	top of Chronozone C5A
322.43	15.27	14.38	base of Chronozone C5B
332.49	16.22	10.59	top of Chronozone C5
344.68	17.57	9.03	top of Chronozone C5D
353.94	18.56	9.35	top of Chronozone C5E
362.73	19.35	11.13	top of Chronozone C6
375.39	20.45	11.51	base of Chronozone C6n
377.24	20.61	11.51	extrapolation to unconformity
377.241	21.59	0	
378.87	21.71	13.66	extrapolation to unconformity
390.62	22.57	13.66	top of Chronozone C6B
408.23	23.27	25.16	top of Chronozone C6n3
419.74	24.21	12.25	base of Chronozone C6n1
			extrapolate to 430.01 msb

represented [Clement and Robinson, 1986]. The only major exceptions are that (1) Chronozone C5ACr is not identified because this interval is represented by coring gaps (Figure 1); and (2) the base of Chronozone C5n is not clear (Figure 1).

Biostratigraphy

We examined one to seven samples per core (9.5 m) from cores 25 (lower upper Miocene) to 46 (uppermost Oligocene) for first and last occurrences of diagnostic planktonic foraminifera. Low-latitude zonal marker species are rare at this location, and the initial shipboard biostratigraphy reported only coarse planktonic foraminiferal biostratigraphy because of the scarcity of low-latitude taxa [Ruddiman et al., 1986b]. Examination of large samples (20-30 cm^3) revealed rare occurrences of many low-latitude marker species. We used the species concepts of Kennett and Srinivasan [1983] and Bolli and Saunders [1985] and the zonal scheme of Kennett and Srinivasan [1983](Figure 1). Details of the planktonic foraminiferal biostratigraphy will be presented elsewhere [J. Zhang et al., manuscript in preparation, 1990]. We compare the first and last occurrences of critical marker species with the magnetochronology (Figure 1) to evaluate latitudinal diachrony.

Isotope Stratigraphy

Samples for isotope analyses were soaked in hydrogen peroxide and sodium metaphosphate, washed with sodium metaphosphate in tap water through a 63-μm sieve, and air-

dried. Foraminifera were ultrasonically cleaned in distilled water for 2-10 s. Oxygen and carbon isotope studies were performed on the benthic foraminifera *Cibicidoides* spp. (see methods of Miller et al. [1989] and Wright and Miller [1990]). The Site 608 stable isotope data will be tabulated elsewhere [Wright et al., 1990 and manuscript in preparation, 1990].

Sr isotope studies were performed on more than 200 specimens of mixed planktonic foraminiferal taxa picked from the greater than 150-μm size fraction and dissolved in 1.5 N HCl. Standard ion exchange techniques [e.g., Hart and Brooks, 1974] were used to separate strontium for analysis on a VG Sector mass spectrometer at Rutgers University. Internal precision (intrarun variability) on the Sector is approximately ±0.000008 (mean 2σ error for 69 analyses at Site 608; Table 2); external precision (interrun variability) is approximately ±0.000030 or better (see discussion section). At Rutgers, NBS 987 is routinely measured as 0.710252 (2 σ standard deviation 0.000026; n = 35) normalized to $^{86}Sr/^{88}Sr$ of 0.1194. DePaolo and Ingram [1985] and DePaolo [1986] report values for NBS 987 of 0.710310; therefore, we subtracted 0.000058 from the data of DePaolo [1986] to facilitate comparisons with our data from Site 608. Richter and DePaolo [1988] similarly report values for NBS 987 of 0.710330; therefore, we subtracted 0.000078 from their data. Other than this adjustment for differences in standards, our data routinely compare well with data from other labs [Miller et al., 1988].

Foraminifera are well preserved in the Miocene section at Site 608. There is no optical evidence of diagenetic overgrowths or obvious replacement of the calcite tests. Our stable isotope measurements at Site 608 compare well with records from other locations [Miller et al., 1986; Wright and Miller, 1990]. In particular, the Miocene oxygen isotope record at Site 608 has a similar amplitude and character as coeval records from the western North Atlantic Site 563 [Miller and Fairbanks, 1985; J.D. Wright et al., manuscript in preparation, 1990], equatorial Pacific Site 289 [Woodruff et al., 1981; Savin et al., 1981], and high-latitude Indian Ocean Site 747 [Wright and Miller, 1990]. The similarity among records with different burial histories argues against the diagenetic alteration of the Site 608 record (see discussion section).

RESULTS

Biostratigraphy

Planktonic foraminiferal biostratigraphy confirms the overall interpretation of the Miocene magnetochronology presented in Figure 1. No obvious hiatuses are indicated by foraminiferal biostratigraphy. We estimate ages of planktonic foraminiferal first and last occurrences by interpolating ages between magnetochronozonal boundaries; derivation of age estimates in this manner is termed magnetochronology [Berggren and Van Couvering, 1974]. Magnetochronologic

TABLE 2. Sr Isotope Data, Site 608

Sample	Age, Ma	Depth, msb	$^{87}Sr/^{86}Sr$	Error
22-4, 80-84	8.27	197.20	0.708878	0.000013
22-4, 80-84	8.27	197.20	0.708997	0.000006
23-3, 88-93	8.34	198.78	0.708878	0.000014
24-4, 73-78	9.30	219.33	0.708920	0.000014
25-2, 33-38	9.61	225.53	0.708942	0.000007
26-1, 78-83	10.05	234.08	0.708934	0.000007
27-1, 3-8	10.50	242.93	0.708884	0.000004
28-1, 90-95	11.03	253.40	0.708847	0.000017
28-1, 90-95	11.03	253.40	0.708927	0.000006
29-3, 64-67	11.67	265.75	0.708891	0.000004
29-5, 50-53	11.84	268.60	0.708852	0.000006
29-5, 50-53	11.84	268.60	0.708845	0.000006
30-1, 128-132	12.09	272.98	0.708853	0.000005
30-3, 15-20	12.20	274.85	0.708891	0.000018
30-3, 15-20	12.20	274.85	0.708874	0.000010
30-3, 15-20	12.20	274.85	0.708877	0.000013
30-5, 22-26	12.38	277.96	0.708838	0.000006
31-2,75-78	12.71	283.55	0.708978	0.000008
31-2, 75-78	12.71	283.55	0.708816	0.000005
31-3, 68-73	12.79	284.98	0.708848	0.000006
31-5, 68-73	12.94	287.98	0.708899	0.000008
32-1,80-85	13.11	291.70	0.708853	0.000006
32-1, 80-85	13.11	291.70	0.708844	0.000005
32-3, 131-135	13.33	295.21	0.708823	0.000005
32-5, 80-86	13.53	297.70	0.708824	0.000013
32-5, 80-85	13.53	297.70	0.708828	0.000018
33-1, 78-83	13.80	301.28	0.708888	0.000011

TABLE 2. cont.

Sample	Age, Ma	Depth, msb	$^{87}Sr/^{86}Sr$	Error
33-2, 47-50	13.88	302.47	0.708929	0.000004
33-CC	13.98	303.90	0.708843	0.000007
34-2, 109-111	14.49	311.19	0.708822	0.000004
34-4, 105-110	14.80	315.65	0.708760	0.000026
34-4, 105-110	14.80	315.65	0.708800	0.000006
34-6, 110-115	15.01	318.70	0.708742	0.000006
35-1, 110-115	15.16	320.80	0.708772	0.000004
35-3, 115-120	15.40	323.85	0.708777	0.000006
36-1, 90-95	16.00	330.20	0.708745	0.000005
36-3, 92-97	16.30	333.22	0.708788	0.000006
36-5, 100-105	16.64	336.30	0.708776	0.000005
37-3, 100-105	17.37	342.90	0.708679	0.000004
37-5, 110-115	17.70	345.90	0.708714	0.000011
38-1, 66-71	18.05	349.16	0.708639	0.000021
38-3, 69-74	18.37	352.19	0.708699	0.000005
38-3, 69-74	18.37	352.19	0.708691	0.000005
38-5, 73-78	18.68	355.23	0.708647	0.000006
39-1, 70-75	19.00	358.80	0.708585	0.000006
39-3, 17-22	19.22	361.27	0.708577	0.000006
39-CC	19.47	364.10	0.708539	0.000006
40-2, 85-90	19.99	370.05	0.708518	0.000006
40-2, 85-90	19.99	370.05	0.708520	0.000006
40-4, 117-122	20.28	373.47	0.708445	0.000006
40-4, 117-122	20.28	373.47	0.708458	0.000006
40-CC	20.58	376.30	0.708437	0.000007
41-2, 92-97	21.05	379.72	0.708453	0.000008
41-4, 107-112	21.49	382.87	0.708398	0.000006
42-1, 100-105	22.19	387.90	0.708386	0.000005
42-3, 100-105	22.58	390.90	0.708366	0.000004
42-3, 100-105	22.58	390.90	0.708379	0.000011
42-5, 86-91	22.69	393.76	0.708351	0.000007
43-1, 115-120	22.85	397.65	0.708392	0.000007
43-3, 110-115	22.97	400.60	0.708345	0.000005
43-3, 110	22.97	400.60	0.708379	0.000011
43-5, 10-15	23.05	402.60	0.708317	0.000007
44-2, 10-15	23.25	407.70	0.708295	0.000005
44-4, 7-12	23.52	411.30	0.708311	0.000004
45-1, 38-40	23.91	416.08	0.708290	0.000005
45-4, 38-40	24.28	420.58	0.708245	0.000005
46-1, 38-40	24.70	425.68	0.708226	0.000007
46-4, 21-23	25.05	430.01	0.708211	0.000010

age estimates of first and last occurrences do not involve circular reasoning, because once the magnetostratigraphy is placed into a general time frame and the section is shown to be continuous, the law of superposition allows the ordinal pattern matching of the Site 608 record to the GPTS.

The magnetochronologic age estimates for many of the Miocene taxa compiled by Berggren et al. [1985] were derived from Atlantic Sites 516 (30°S)[Berggren et al., 1983a,b], 563 (33°N), and 558 (38°N)[Miller et al., 1985]. Several low latitude markers display first and last occurrences which are apparently synchronous between these locations and Site 608.

1. *Neogloboquadrina acostaensis* first occurs at the base of Chronozone C5n (~10.4 Ma) at Sites 563 and 558; at Site 608, it first occurs at the base of a similar thick normal polarity interval identified as Chronozone C5n (Figure 1). Still, we caution that the magnetochronologic interpretation of the section immediately below this is uncertain.

2. *Globigerina nepenthes* first occurs near the base of Chronozone C5r at Sites 563 and 608 (ca. 11.3 Ma).

3. *Praeorbulina sicanus* first occurs in the middle of Chronozone C5Cn at Sites 563 and 608 (ca. 16.6 Ma).

4. The LO of *Catapsydrax dissimilis* is at the top of Chronozone C5Dr at Site 608 (~18.1 Ma); at Sites 516 and 558, this taxon last occurs within C5Dn [Berggren et al., 1983a,b] with an age estimate of 17.6 Ma [Berggren et al., 1985]. This uncertainty of 0.5 m.y. is within the sampling resolution at Site 608, because there is only one sample in Chronozone C5Dn.

5. *Orbulina suturalis* first occurs at Site 608 in Chronozone C5ADr (~14.8 Ma); this species has been firmly calibrated as first occurring in Chronozone C5Bn at several locations (15.2 Ma)[Berggren et al., 1985]. This uncertainty of 0.4 m.y. is within the sampling resolution at Site 608.

6. *Globoquadrina dehiscens* first occurs at Site 608 near the top of Chronozone C6Cn (23.5 Ma); at several other locations this taxon first occurs near the base of C6Br (23.2 Ma).

Three species display notably delayed first and last occurrences:

1. *Globorotalia peripheroacuta* first occurs in Chronozone C5ACn at Site 608 (~14.0 Ma); elsewhere this taxon first occurs in Chronozone C5Bn (14.9 Ma)[Berggren et al., 1985]. There is a coring gap at this level at Site 608, and the resulting first occurrence could be 0.5 m.y. older. Still, it would not be surprising if this member of the *G. fohsi* lineage has a delayed FO at Site 608, because *G. fohsi* ssp. are represented at Site 608 by only a solitary occurrence of *G. fohsi lobata* (Figure 1).

2. *Globorotalia kugleri* last occurs in upper Chronozone C6Bn at Site 608 (ca. 22.7 Ma). This is 0.9 m.y. older than the 21.8 Ma LO reported by Berggren et al. [1985].

3. *Globorotalia praescitula* first occurs in C5En at Site 608 (~19.0 Ma). This is 1.3 m.y. older than its reported calibration at Site 516 [Berggren et al., 1983a,b, 1985]. The magnetostratigraphic interpretation of this interval at Site 516 is not clear. The magnetostratigraphy is straightforward at this level at Site 608; therefore, we believe that the age estimate at Site 608 is valid for the true first appearance of this taxon.

The LO of *Globorotalia mayeri* is juxtaposed with the FO of *N. acostaensis* at Site 608 (Figure 1), as it is at Sites 563 and 558. Therefore, Zone N15 is effectively absent at these locations. We previously ascribed the absence of this zone to the diachronous LO of *G. mayeri*, with it disappearing later at higher latitudes [Miller et al., 1985]. Alternatively, there may be a hiatus at this level at Sites 563, 558, and 608. We argued that there is no hiatus at this level at Site 563 because the magnetostratigraphic record appears to be complete; still, there is a coring gap at Site 563 within Chronozone C5 [Miller et al., 1985]. The Site 608 record is not clear in this interval. The LO of *G. mayeri* occurs in a normal interval in lower Core 26 to upper Core 27 below the thick normal interval of Core 23 to uppermost Core 26. The normal polarity interval contained in lower Core 26 to upper Core 27 does not appear to match the GPTS of Berggren et al. [1985]. However, McDougall et al. [1984] noted that a short interval of reversed polarity occurred near the base of Chronozone C5n in Iceland, similar to the record at Site 608. This short reversed polarity interval observed in lavas and sediments may reflect a polarity change not discerned in the seafloor record. Further magnetostratigraphic studies are needed to evaluate the nature of the GPTS during Chron C5, the validity of Zone N15 at higher latitudes, the possible diachrony of the LO of *G. mayeri*, and the possibility of a widespread hiatus at this level.

Sr Isotope Stratigraphy

There is an overall increase in $^{87}Sr/^{86}Sr$ values of 0.000600 from the uppermost Oligocene to lower middle Miocene at Site 608, with values increasing from 0.7082 to 0.7088 between 430 msb and 335 msb (Figure 1). There is less of a change between this level and the top of the section examined. Between 335 msb and 195 msb, $^{87}Sr/^{86}Sr$ values increase by less than 0.000200 (from 0.7088 to less than 0.7090)(Figure 1). It is not clear if these increases were monotonic or if there are higher-order (e.g., on the 100 kyr scale) variations. Our average sampling interval is 0.3 m.y., and thus we are unable to discern changes on a scale finer than about 1 m.y.

The causes of changing $^{87}Sr/^{86}Sr$ ratios through time are not well known (see discussion section); therefore, the relationships between Sr isotope variations and age must be empirically determined. We did this by estimating the ages of our $^{87}Sr/^{86}Sr$ measurements at Site 608 using magnetochronology (Table 1); we averaged duplicate analyses and computed linear and higher order regressions.

In determining the $^{87}Sr/^{86}Sr$ changes through time for a single section (Figures 2,3), we chose Sr isotopes values as the dependent variable and age as the independent variable in the regression. (The dependent variable is shown on the abscissa in Figures 2 and 3 to be consistent with previous displays.) Other studies have specified age as the dependent variable in regression analysis [e.g., McKenzie et al., 1988; Miller et al., 1988]. This assumes that there are no errors in Sr isotope measurements. In contrast, we assume that age is well known for the regression of the standard, and that the regression provides a calibration curve which may be inverted to compute ages [Draper and Smith, 1981]. While such an assumption is not valid for many geologic studies, it is warranted in the study of a single section with good magnetochronology since superposition maintains relative age offsets and magneto-chronology provides relatively precise age control. In determining a calibration curve using more than one section, age variables may be inverted due to correlation problems [e.g., Hess et al., 1989]. Therefore, this assumption may not be warranted in this type of two-dependent variable system, and linear regression techniques such as those used by York [1967] may be required.

Draper and Smith [1981] provide an example of a regression analysis similar to ours. In their example [Draper and Smith, 1981, p. 47], the independent variable is provided by age estimates derived from tree rings, and the dependent variable is provided by the corresponding age estimates from radiocarbon measurements. Their regression provides a calibration curve for the radiocarbon measurements (similar to the Sr isotope measurements in this example) relative to the more accurate tree ring ages (similar to the magneto-stratigraphic age estimates in this example). They inverted the regression to compute a calibrated age for a given radiocarbon measurement.

A linear relationship provides an excellent fit for the Site 608 data between 25.1 and 14.7 Ma (Figure 2), with a rate of change of 0.000059/m.y. The linear regression for the interval 25.1-14.7 Ma is in the form

$$^{87}Sr/^{86}Sr = 0.7097091415 - 0.0000596048*(\text{Age, Ma}) \quad (1)$$
$$r = 0.984 \quad s = 0.000034$$

where r is the correlation coefficient and s is the standard error of estimate [Draper and Smith, 1981, p. 207].

To determine the ages of strata by measuring their $^{87}Sr/^{86}Sr$ composition, this equation may be inverted to

$$(\text{Age, Ma}) = 11906.91 - 16777.17*(^{87}Sr/^{86}Sr) \quad (2)$$

Equations (1) and (2) are based on data from 25.1 to 14.7 Ma; we extrapolate these equations into the interval 14.7-14.6 Ma. Thus, these equations are valid from 25.1-14.6 Ma and from 0.708213 to 0.7088389.

A linear regression provides a poorer fit to the Site 608 data between 14.5 and 8.3 Ma because the slope is low,

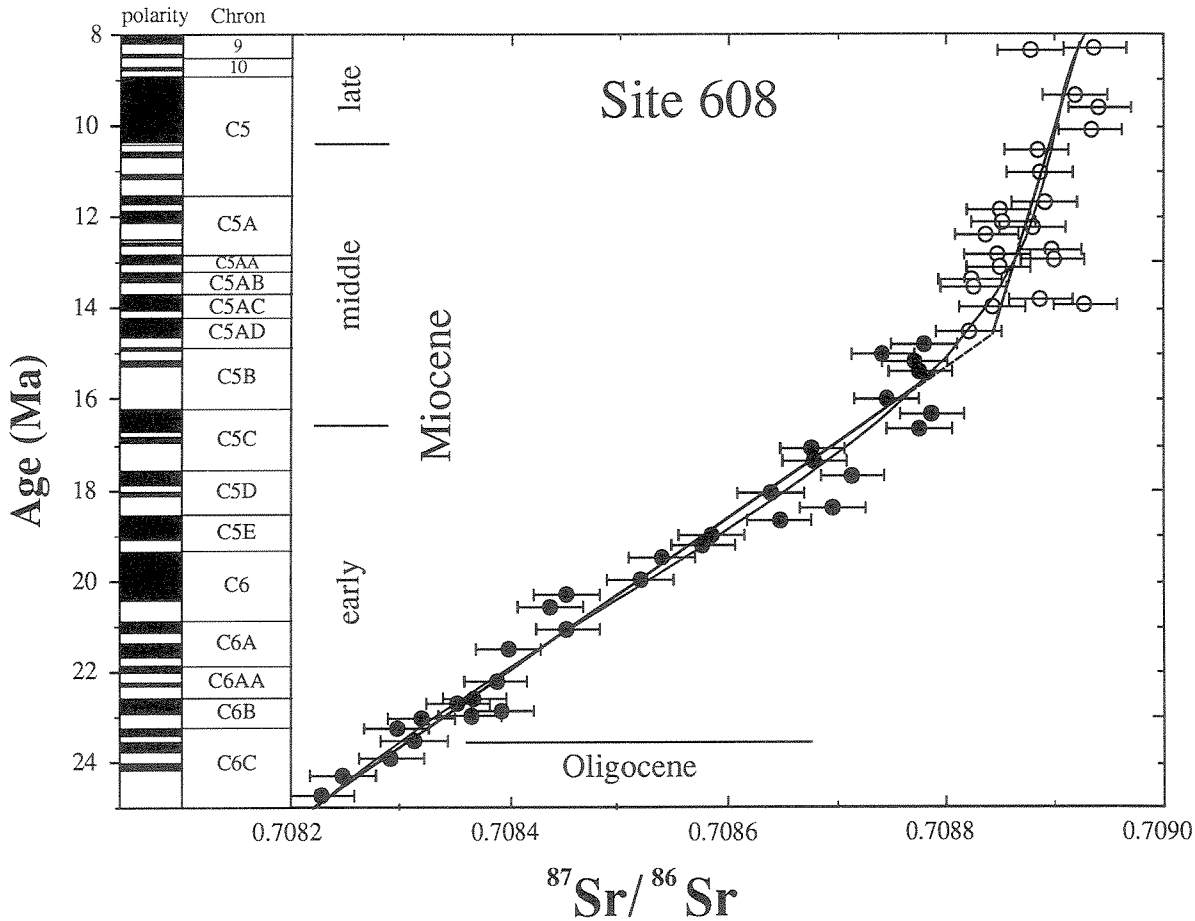

Fig. 2. Sr isotope data versus age, Site 608. Duplicate analyses (Table 2) were averaged and the mean value plotted. Thin line is the fourth- and fifth-order regression through all the data shown. The data were divided into two intervals: 25.1-14.7 Ma (solid circles) and 14.5-8.3 Ma (open circles), and linear regressions were computed for each interval. Error bars given for each point are ±0.000030, our estimate of interrun variability. The time scale is the GPTS of Berggren et al. [1985]. Age were obtained by interpolating between magnetochron boundaries using age model 1 (Table 1).

approaching the errors in measuring $^{87}Sr/^{86}Sr$ (Figure 2). The linear regression for the data from the interval 14.5-8.3 Ma is in the form

$$^{87}Sr/^{86}Sr = 0.70902818 - 0.0000126072*(\text{Age, Ma}) \quad (3)$$
$$r = 0.603 \quad s = 0.000032$$

To determine the ages of "unknown" samples, this equation may be inverted to

$$(\text{Age, Ma}) = 56239.94 - 79319.75*(^{87}Sr/^{86}Sr) \quad (4)$$

We extrapolate equations (3) and (4) to be valid from 14.6 to 8.3 Ma and 0.708844 to 0.708924.

The use of higher-order functions does not significantly improve the fit for either time interval. For example, first- through fifth-order functions for the interval 25.1-14.7 Ma yield correlation coefficients of 0.984, 0.986, 0.989, 0.991, and 0.991, respectively. The overall data between 25.1 and 8.3 Ma are explained well by fourth- and fifth-order functions (r = 0.991 for both, shown as the same line on Figure 2). Nevertheless, the two linear segments shown on Figure 2 provide an excellent approximation of the fourth- and fifth-order functions. Because of the excellent visual fit provided by two linear segments (Figure 2), we use them to approximate the nature of Sr isotope changes for the interval from ca. 25.1 to 8.3 Ma (Figure 2). A higher-order regression provides a significantly better correlation coefficient for the data from about 15 to 8 Ma but does not improve the stratigraphic resolution due to the low rate of change in this interval. Although two linear regressions characterize the data well, we caution (see below) that the inflection point between the regressions (namely, between 16 and 14 Ma) is poorly characterized, and that Sr isotope stratigraphic resolution of this interval is poor.

Sr isotope stratigraphic resolution depends on the rate of change of $^{87}Sr/^{86}Sr$ and the ability to reproduce geologic measurements. External precision of replicate samples is often estimated to be ±0.000020-0.000024 [Hodell et al., 1989, 1990a,b; Hess et al., 1989], although examination of

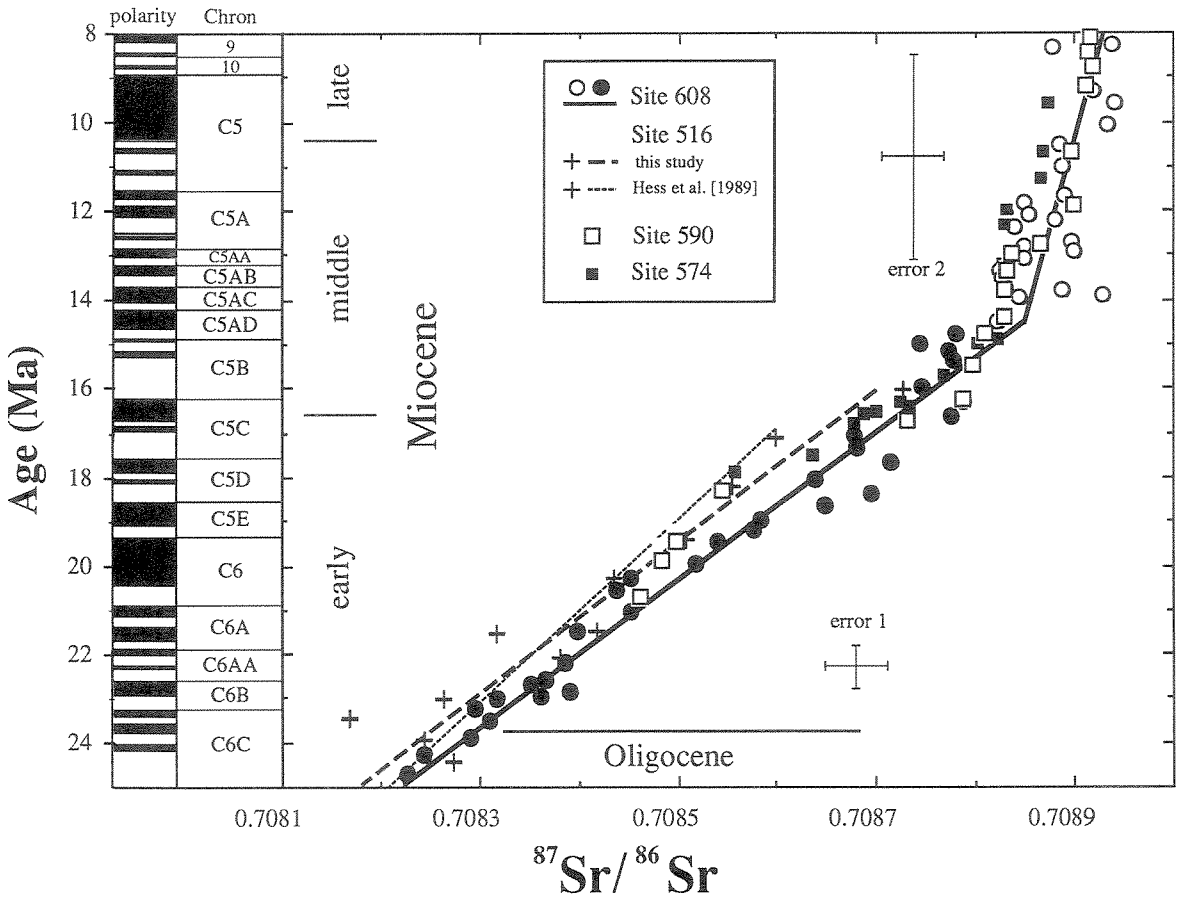

Fig. 3. Comparison of $^{87}Sr/^{86}Sr$ data from Site 608 (circles), Site 590 (open squares; data after DePaolo [1986]), Site 574 (solid squares; data after Richter and DePaolo [1988], and Site 516 (pluses; data after Hess et al. [1986]). Linear regressions were drawn through the Site 608 data from 25.1-14.6 Ma (solid line, closed circles) and from 14.6-8 Ma (solid line, open circles). A linear regression was drawn for the Site 516 data (thick dashed line). The thin dashed line is a regression after Hess et al. [1989]. Horizontal error bars represent our estimate of inter-run variability (±0.000030). Vertical error bars show our estimate of age uncertainties for each regression: ±0.5 m.y. for the older Site 608 regression, and ±2.3 m.y. for the younger regression at Site 608.

geological data generally shows more scatter. We have previously estimated sample reproducibility as ±0.000030 [Miller et al., 1988]. However, our reproducibility may be as good as ±0.000026. This is based on replicate analyses of NBS 987 standard which yield a standard deviation of 0.000026 (2 σ). Still, 15 duplicate samples from Site 608 have mean differences of 0.000035, with 10 duplicates having mean differences of less than 0.000020. Comparison among our Site 608 duplicates provides an overestimate of our uncertainties, because we chose to duplicate samples which deviated the most from the linear regression. We believe that ±0.000030 still provides a conservative estimate of sample reproducibility. With the rate of change of 0.000059/m.y. provided by the 25.1-14.6 Ma regression, ±0.000030 is equivalent to a stratigraphic resolution of ±0.5 m.y. This is our maximum resolution, and does not account for all errors in the regression. With the rate of change of 0.000013/m.y. provided by the 14.6-8.3 Ma regression, ±0.000030 is equivalent to a stratigraphic resolution of worse than ±2.3 m.y.

Residuals are differences between the observed Sr isotope values and values predicted by equations (1) and (3)(Figure 4) which provide a measure of observed errors in the regression models [Draper and Smith, 1981]. The plot of residuals versus the predicted Sr isotope values (Figure 4) shows no trends, indicating that the regression models are adequate [Draper and Smith, 1981, p. 147]. The regression model between 25.1 and 14.7 Ma at Site 608 is based on 33 points with a standard error of estimate of 0.000034 (1σ). Residuals of samples from equation (1)($^{87}Sr/^{86}Sr$ deviations) show that 31 analyses (94%) fall within ±0.000068 as expected (e.g., the residuals/standard error should be <2 for the 95% confidence interval [Draper and Smith, 1981, p. 144]). Residuals of 22 of the 33 points (67%) are within our estimated external precision of ±0.000030 (Figure 4, bottom). With a 2σ standard error of estimate of 0.000068, the equivalent age uncertainties of

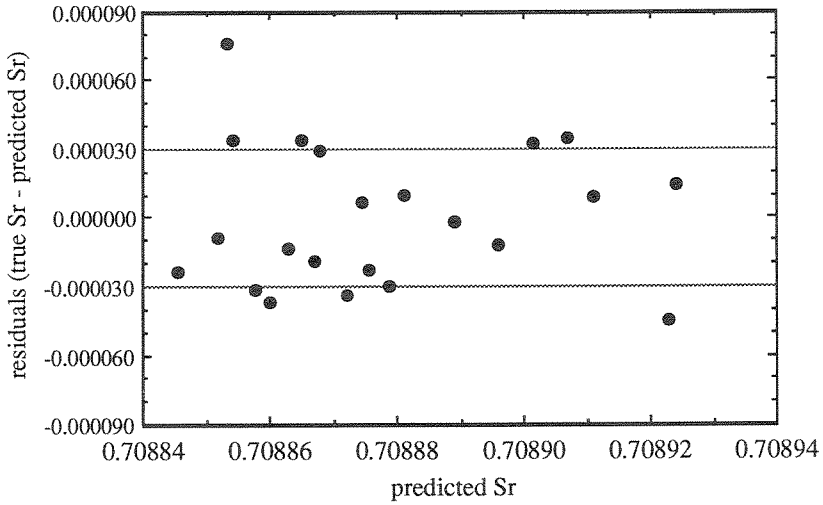

14.6-8.3 Ma regression

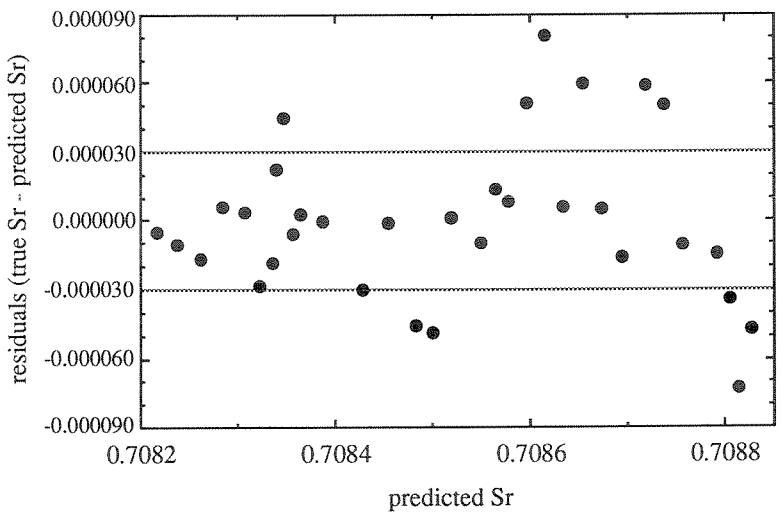

25-14.6 Ma regression

Fig. 4. Residuals of Sr isotope data from equations (1) and (3). These represent the deviations of data from the regression along the $^{87}Sr/^{86}Sr$ axis (Figure 2).

equation (2) may be as high as ±1.15 m.y., although this probably overestimates the total error The regression between 14.5 and 8.3 Ma at Site 608 is based on 22 points with a standard error of estimate of 0.000031. Residuals of samples from the regression ($^{87}Sr/^{86}Sr$ deviations) show that 21 analyses (95%) fall within ±0.000050 and 12 points (55%) are within our estimated external precision of ±0.000030.

Statistics can be used to evaluate errors in ages predicted by Sr isotopes. McKenzie et al. [1988] estimated errors in predicted age for their late Miocene regression; their method is not directly applicable to inverse regression techniques (equations (2) and (4)). The error in predicting age from the Sr isotope regressions may be computed in a manner similar to McKenzie et al. [1988] for inverse regression using the equation provided by Draper and Smith [1981, p. 49]:

$$\text{Age (upper, lower)} = \frac{\text{Age}_0 + (\text{Age}_0 - \overline{\text{Age}})g \pm \frac{ts}{b_1}\sqrt{\frac{(\text{Age}_0 - \overline{\text{Age}})^2}{\Sigma(\text{Age}_i - \overline{\text{Age}})^2} + \frac{1-g}{n}}}{(1-g)} \quad (5)$$

where Age_0 is the predicted age, s is the standard error, t is Student's statistic, b_1 is the slope, $\overline{\text{Age}}$ is the mean age of the regression, n is the number of measurements in the regression, and $g = (t^2s^2)/b_1^2\,\Sigma(\text{Age}_i - \overline{\text{Age}})$.

When the inverse regression is well determined and b_1 is large, g is small and may be approximated as zero [Draper and Smith, 1981]. This approximation is valid for the regression

from 25.1 to 14.7 Ma at Site 608. With a slope of 0.0000596, standard error of 0.0000349, t statistic of 1.96 for 95% confidence interval and 32 degrees of freedom, and $\sum(Age_i - \overline{Age})^2$ of 302.28, equation (5) suggests that equation (2) has an uncertainty of ±0.20 m.y. (for values close to the mean age of 19.9 Ma) to ±0.41 m.y. (for values close to the endpoints of the regression). This assumes that the Sr isotope measurements represent the true value [Draper and Smith, 1981] and thus underestimates the total uncertainty. Equation (5) may be reformulated in which Sr isotope measurements are not true mean values, but as a mean of q observations:

Age (upper, lower) =

$$Age_0 \pm \frac{ts}{b_1}\sqrt{\frac{(Age_0 - \overline{Age})^2}{\sum(Age_i - \overline{Age})^2} + \frac{1}{q} + \frac{1}{n}} \qquad (6)$$

This again assumes g is approximately 0. For a single Sr isotope measurement of an "unknown," equation (6) suggests equation (2) has an uncertainty at the 95% confidence interval of ±1.16 for values close to the mean and ±1.2 m.y. for values close to the end points. (We subsequently round the errors and report uncertainties for values close to the mean and close to the endpoints as one number.) The 80% confidence interval has corresponding uncertainties of ±0.8 m.y. A greater number of measurements of Sr isotopes "unknowns" greatly improves statistical uncertainties. For example, given the mean of three measurements at one stratigraphic level (q = 3), uncertainties are ±0.7 m.y. (95% confidence interval), ±0.6 m.y. (90% confidence interval), and ±0.5 m.y. (80% confidence interval).

The regression from 14.6 to 8.3 Ma has a low slope (b_1 is small) and is poorly determined; in such cases, inverse regression techniques may not be practical [Draper and Smith, 1981]. We therefore place little emphasis on our ability to correlate strata using equations (3) and (4)(from about 15 to 8 Ma).

We compare the Site 608 Sr isotope record with previously published Miocene $^{87}Sr/^{86}Sr$ records: western South Atlantic Site 516 [Hess et al., 1986, 1989], western South Pacific Site 590 [DePaolo, 1986], and central Pacific Site 574 [Richter and DePaolo, 1988](Figure 3). The early Miocene Site 516 data show greater scatter than the Site 608 data (Figure 3). Six out of the 12 points between 25 and 16 Ma at Site 516 fall outside ±0.000030 of the regression through those points (Figure 3). In contrast, 22 out of 33 points between 25.1 and 14.7 Ma at Site 608 fall within ±0.000030 of the regression through those points (Figure 4, bottom). The 516 regression of Hess et al. [1989](thin dashed lines, Figure 3) is offset from the Site 608 regressions by as much as 0.000090 (Figure 2). We ascribe this large difference to correlation problems at Site 516. Although this site was analyzed for magnetostratigraphy, the identification of the magnetochronozones is largely dependent on biostratigraphy [Berggren et al., 1983a,b]. We revised the age model for this site. The revised regression (thick dashed line, Figure 3) of the Site 516 data is only about 0.000030 different from the Site 608 regression.

There is good agreement in $^{87}Sr/^{86}Sr$ records between Sites 608 and 590 from 12 to 8 Ma and from 17 to 15 Ma (Figure 3). From ca. 21 to 18 Ma and 15 to 12 Ma (Figure 3), the Site 590 data appear to be lower than coeval values at Site 608 by 0.000005 to 0.000060. However, the biostratigraphic control at Site 590 is uncertain, and we ascribe these changing offsets between the Sr isotope records at Sites 590 and 608 to biostratigraphic problems. Similarly, there is good agreement between Sites 574 and 608 from 18 to 14 Ma, but $^{87}Sr/^{86}Sr$ values at Site 574 are lower than coeval values at Site 608 from 12 to 9 Ma by approximately 0.000020 to 0.000050 (Figure 3). We again attribute this to biostratigraphic uncertainties in the Site 574 correlations.

Miller et al. [1988] developed a single regression for the late Eocene to earliest Miocene, which they believed to be valid from 38 to 22 Ma. Hess et al. [1989] provided two late Eocene to early Miocene $^{87}Sr/^{86}Sr$ age regressions based partly on western North Atlantic Site 563, eastern South Atlantic Site 529, and Site 516. Their first regression is for the late Eocene to late Oligocene (ca. 37-26 Ma). Their second regression is for the latest Oligocene to middle Miocene interval (26-16 Ma; shown on Figure 3) and is largely based on data from Site 516. Considering the scatter and problems in correlation of the Site 516 record, we believe that the Site 608 regression provides a better representation of $^{87}Sr/^{86}Sr$ changes during the early Miocene (Figure 2).

Hess et al. [1989] suggested that there was a systematic $^{87}Sr/^{86}Sr$ offset between their sites and data from Site 522 [Miller et al., 1988]. They ascribed the lower $^{87}Sr/^{86}Sr$ values at Site 522 to diagenesis. These differences are not significant. Comparison of the regressions obtained by Hess et al. [1989] and Miller et al. [1988] shows good agreement during the late Eocene to "middle" Oligocene (Figure 5)(ca. 37-30 Ma). The only major differences between the studies are in the late Oligocene to early Miocene, as discussed above.

Late Eocene to early late Miocene (~38-8 Ma) $^{87}Sr/^{86}Sr$ variations are represented well by three regressions (Figure 5)(equations (1) and (3) and equation (1) of Miller et al. [1988]). During the middle Eocene (52-41 Ma; Figure 5), there was variability of about ±0.000075, but there was no apparent trend [Hess et al., 1986]. Although the three regressions (Figure 5) appear to be valid for most of their age ranges, the inflection points in the $^{87}Sr/^{86}Sr$ record between the regressions are poorly constrained:

1. A moderate rate of increase began near middle/late Eocene boundary. At Site 516 this increase began between 588 and 627 msb (Figure 5)[Hess et al., 1986]. *Acarinina spinulosa* (41.1 Ma) last occurs at Site 516 at 633 msb, while *Turborotalia cerroazulensis* (36.6 Ma) last occurs at 538 msb [Pujol, 1983]. With this coarse biostratigraphic control, the change in slope has an estimated age of 40.8-38.9 Ma.

2. Miller et al. [1988] estimated that their Oligocene regression was valid until the early Miocene (ca. 22 Ma). In contrast, Hess et al. [1989] suggested that the rate of change of $^{87}Sr/^{86}Sr$ increased during the late Oligocene. Hess et al. [1989] were correct. Comparison of the records from Sites 522 and 608 shows that the change in slope occurred during the late Oligocene (~25-24 Ma)(Figure 5).

3. Equation (1) is valid for the early Miocene to the earliest middle Miocene (from 25.1 to 14.7 Ma). Equation (3) appears to be valid beginning in the middle Miocene (14.5 Ma). We have no data in the interval 14.7-14.5 Ma and extrapolate equations (1) and (3) into this interval. Apparently, there was greater variability in the Site 608 record from 16 to 14 Ma (Figure 4, bottom), and we caution that equation (1) may have greater uncertainties in the interval 16-14.6 Ma (dashed line in Figure 2) than it does prior to this.

4. McKenzie et al. [1988] and Hodell et al. [1989, 1990a,b] described a large rate of increase during the latest Miocene. Again, the precise timing of the inflection point is difficult to constrain, because the former suggested that it began at about 6 Ma, while the latter suggested that the increase began at 5.5 Ma.

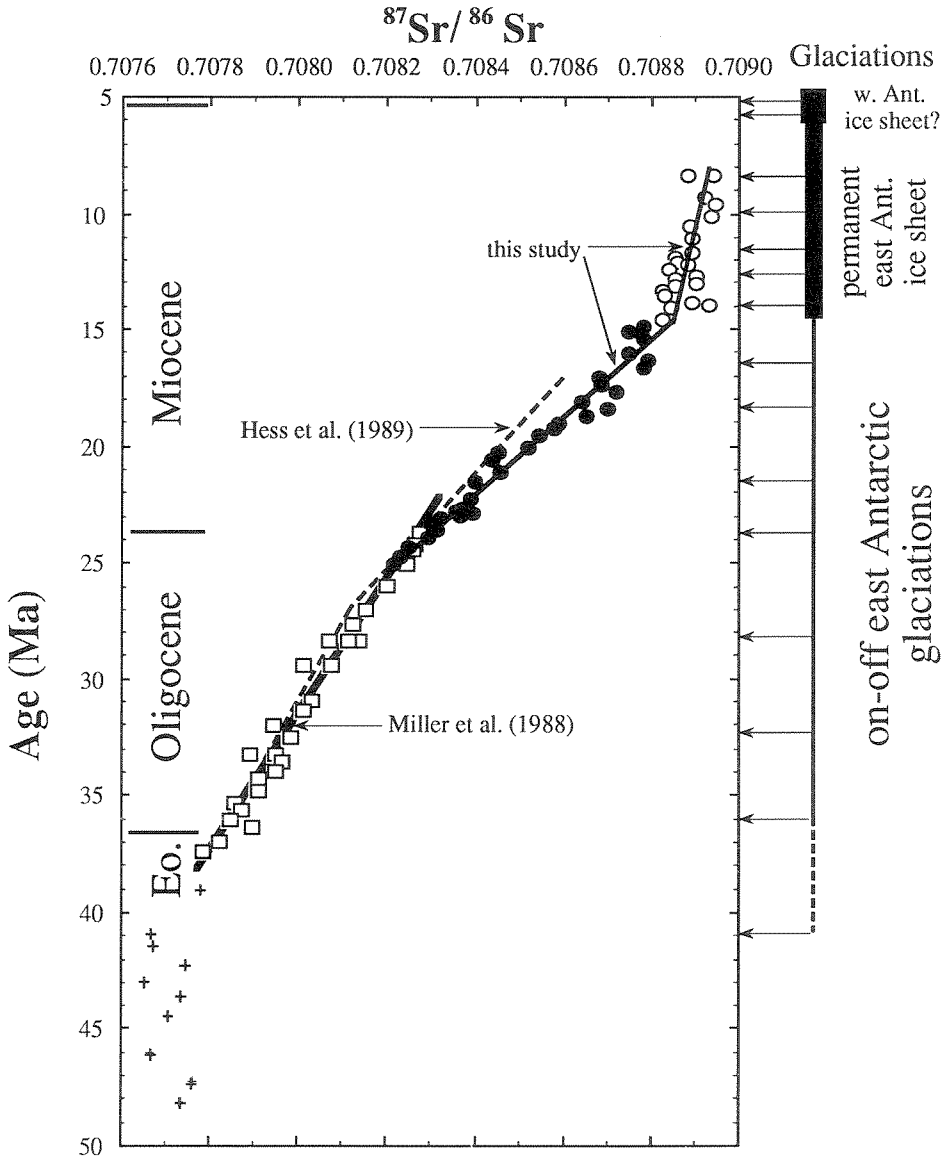

Fig. 5. Summary of $^{87}Sr/^{86}Sr$ evolution from the late middle Eocene to early late Miocene. Data are shown from Site 516 (49-38 Ma only; pluses; Hess et al. [1986]), Site 522 (38-22 Ma; open squares; Miller et al. [1988]), and Site 608 (25.1-8 Ma; circles, this study). Linear regression from equation (1) of Miller et al. [1988] and equations (1) and (3) of this study are shown as solid lines. The linear regressions of Hess et al. [1989] are shown for comparison (dashed line). Arrows under glaciations indicate individual inferred ice growth events.

Stable Isotope Stratigraphy

Savin et al. [1975] and Shackleton and Kennett [1975] observed that large (>1.0 ‰) benthic foraminiferal $\delta^{18}O$ increases occurred near the Eocene/Oligocene boundary and in the middle Miocene. Various studies established that these increases are magnetobiostratigraphically synchronous among ocean basins, and therefore can be used for correlation [Keigwin, 1980; Corliss et al., 1984; Oberhansli et al., 1984; Miller et al., 1985, 1988; Savin et al., 1981; Woodruff et al., 1981; Miller and Fairbanks, 1985; Vincent et al., 1985; etc.]. We recently focused on other Cenozoic $\delta^{18}O$ variations, both large (>1.0 ‰) and small (~0.5 ‰), which similarly provide potential for stratigraphic correlations. Miller et al. [1990a] and Wright and Miller [1990] showed that 12 Oligocene-Miocene benthic foraminiferal $\delta^{18}O$ increases are synchronous within the resolution of magnetobiostratigraphy. They used these $\delta^{18}O$ increases to define stable isotope zones. The bases of the zones are recognized by the maximum $\delta^{18}O$ values. Alphanumeric names are given to the zones numbering from the base of the Oligocene (Oi zones) and the base of the Miocene (Mi zones).

The early to early late Miocene $\delta^{18}O$ increases and their associated zones (i.e., Mi1, Mi1a, Mi1b, M12, Mi3, Mi4, Mi5, Mi6, and Mi7) are well-defined at Site 608 (Figure 6). Magnetostratigraphy indicates that these increases are synchronous with increases at western Atlantic Site 563 and Indian Ocean Site 747 [Miller et al., 1990a; Wright and Miller, 1990].

Wright and Miller [1990] used oxygen isotope correlations to revise the magnetochronologic interpretation of the lowermost Miocene at Site 608. The $\delta^{18}O$ increase associated with Zone Mi1 occurs at ~410 msb at Site 608, while the increase associated with Zone Mi1a occurs at ~378 msb (Figure 6). The former increase correlates with Chronozone C6Cn3-n2 at Site 522 [Miller et al., 1990a], while the latter increase correlates with uppermost Chronozone C6Ar at Sites 747 and 563. Based on these correlations, Wright and Miller [1990] interpret a normal magnetozone between 391 and 398 msb as C6Bn, not C6A as previously interpreted [Clement and Robinson, 1986; Miller et al., 1986]. Wright and Miller [1990] suggest that Chronozones C6An and C6 are concatenated, not Chronozones C6C and C6B as previously interpreted. Other than this, the record at Site 608 is interpreted as a relatively complete magnetochronology (i.e., chronozones are interpreted by counting up from C5E to C5). These interpretations are supported by biostratigraphy (see above). Although the revised isotope correlation does not

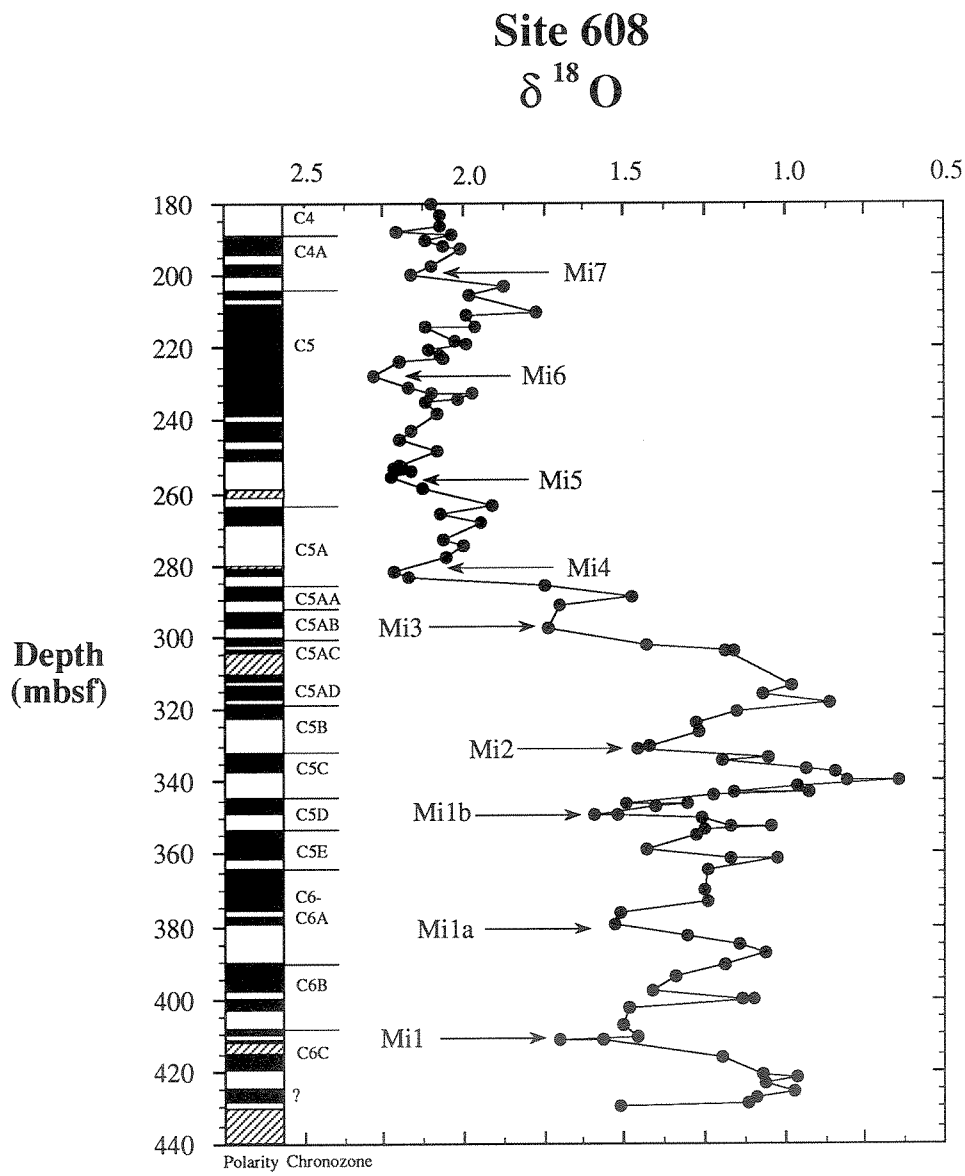

Fig. 6. Oxygen isotope data, Site 608 plotted versus magnetochronozones. All data were measured on *Cibicidoides* spp. The maxima used to defined the bases of oxygen isotope Zones Mi1-Mi7 are indicated with arrows.

greatly change the age interpretations, it emphasizes that integration of biostratigraphy, magnetostratigraphy, and isotope stratigraphy provides the clearest stratigraphic correlations.

DISCUSSION

Stratigraphic Reference Sections

A stratigraphic reference section provides a chronostratigraphic standard in which various records (including isotopes, biostratigraphy, and magnetostratigraphy) are directly correlated with one another. Stratigraphic reference sections are not formal stratotypes, but serve a similar function. The deep-sea sections we chose are more continuous than traditional stratotypes, which are generally unconformably bound sections and only represent a glimpse of the stratigraphic record. The International Commission on Stratigraphy [Hedberg, 1976; Cowie, 1986; Cowie et al., 1989] encouraged the development of formal boundary stratotypes which are generally located in deep-sea sediments exposed on land. These outcrops provide the continuous deposition and pelagic biostratigraphy needed for stratigraphic reference, but often suffer from diagenetic changes which alter the isotope records. For example, the recently approved Eocene/Oligocene boundary stratotype near Massignano, Italy contains good magnetostratigraphy, biostratigraphy, and radioisotope age measurements, but the oxygen isotope record is severely overprinted by diagenesis [Premoli-Silva et al., 1988]. Site 522 provides the geochemical reference section for the Eocene/Oligocene boundary interval [Poore and Matthews, 1984; Oberhansli and Toumarkine, 1985; Miller et al., 1988] that is directly correlated to the boundary stratotype using magnetobiostratigraphy [Poore et al., 1982; Tauxe et al., 1983, 1984].

Pleistocene oxygen isotope correlations have relied on reference sections. Piston core V28-238 serves as an upper Pleistocene reference section unifying magnetostratigraphy and isotope stratigraphy [Shackleton and Opdyke, 1973]. Later studies produced a composite stack from several sections for an upper Pleistocene oxygen isotope reference [Imbrie et al., 1984]; this was possible because the known Milankovitch forcing allowed precise correlation of records. The oxygen isotope standard has actually supplanted the stratotype as a reference for late Pleistocene marine correlations. For the pre-Pleistocene, reference sections such as Site 522 (latest Eocene-Oligocene) and Site 608 (early Miocene to early late Miocene) can work in concert with unit and boundary stratotypes, providing the requisite complete isotope records not obtainable from the stratotypes.

Site 608 provides an isotope reference section which can be tested. Isotope records from other sections must be compared with Site 608 to verify that this section properly represents global isotope changes. The difference between single and stacked composite sections is emphasis, and the results of these two approaches often are the same. For example, the late Eocene-early Oligocene portion of the Sr isotope calibration is the same between our Site 522 record and the stacked composite of Hess et al. [1989](Figure 5). Still, stacking multiple sections adds an additional source of error: problems in age correlations. Thus, we prefer to develop one section for a reference and to compare it with other sections to verify its validity.

A good stratigraphic reference section should permit direct correlation to the GPTS and precise age estimates, although these age estimates are only as accurate as the calibration of the GPTS. However, any future recalibration of the age of the GPTS will not compromise isotope-polarity correlations at the reference section, and new age estimates may be readily obtained. For example, there has been considerable discussion that the age of the Eocene/Oligocene boundary may be closer to 34 Ma [Premoli-Silva et al., 1988] than the 36.6 Ma estimated by Berggren et al. [1985]. Recalibration of the boundary age may require changes to the Eocene and Oligocene GPTS, which would result in different ages for isotope fluctuations. Nevertheless, the reference section at Site 522 provides a firm calibration of oxygen, carbon, and Sr isotope changes with polarity history [Miller et al., 1988]. Changing the age of the boundary will not change the fact that a major oxygen isotope increase occurred in earliest Oligocene Chron C13n [Miller et al., 1988]; only the age estimate of Chron C13n and the associated oxygen isotope increase will change.

Diagenesis

Richter and DePaolo [1988] argued that diagenesis is widespread among Cenozoic sections. They noted that $^{87}Sr/^{86}Sr$ offsets of 0.000060 occur between apparently coeval levels at Sites 574 and 590 and ascribed these differences to diagenetic alteration. These Sr isotope differences may be explained by biostratigraphic uncertainties. We believe that, although diagenesis is certainly a problem in some sections, Richter and DePaolo present an overly pessimistic view. Many studies have demonstrated that sections with different burial histories yield similar Sr isotope values for coeval levels [Hess et al., 1986; Miller et al., 1988; Hodell et al., 1989]. For example, the Sr isotope record of the indurated Contessa Quarry section yields similar values to those from the shallowly buried coeval section at Site 522 [Miller et al., 1988]. Ludwig et al. [1988] report Sr isotope stratigraphy from carbonate sections with shallow burial diagenesis which appear to yield reliable age estimates.

The debate over the importance of diagenesis on sediment isotopes is not new. Killingley [1983] ascribed the general Cenozoic $\delta^{18}O$ increase to increased diagenesis with age. Miller et al. [1987] argued that Killingley's model failed to explain not only the overall trend but also correlatable fluctuations recorded at diverse locations with different burial histories. We similarly show that the Site 608 oxygen isotope record yields virtually identical values to coeval records from the western Atlantic, Pacific, and Indian oceans, all of which have different burial depths and histories. Based on the similarities in both Sr and oxygen isotope records among locations, we suggest that diagenesis is minor for most shallowly (<400 m) buried deep-sea sections.

The Sr isotope record is apparently less susceptible to diagenetic alteration than the oxygen isotope record. Hess et al. [1986] noted that the Sr isotope records from the Campanian-Maestrichtian at Site 305 and the Eocene at Site 366 may have been diagenetically altered, as shown both by optical evidence and low Sr/Ca ratios. Eocene Sr isotope values at Site 366 are similar to coeval values elsewhere, suggesting that this section records unaltered Sr isotope values [Hess et al., 1986]. However, we have shown that the upper Eocene to lower Oligocene oxygen isotope record at Site 366 is overprinted by diagenetic alteration, with the values approximately 0.5 ‰ lower than expected from coeval sections [Miller et al., 1989]. We suggest that oxygen isotopes potentially provide one means of screening deep-sea sections for Sr isotope diagenesis, supplementing existing techniques

(e.g., Sr/Ca ratios, [Graham et al. 1982; Hess et al. 1986]. Sr isotopes may be assumed to be unaltered if the oxygen isotope records can be shown to yield expected values (i.e., equivalent to coeval deep-sea sections). If the oxygen isotope record is altered, the Sr isotope record may or may not yield stratigraphically useful values.

Causes of Sr Isotope Fluctuations

Elderfield [1986] provides an excellent review of Sr isotope principles and possible causal mechanisms for oceanic Sr isotope changes. Oceanic $^{87}Sr/^{86}Sr$ ratios reflect the balance between two geochemical reservoirs, oceanic crust (~0.703) and continental crust (~0.712). Hydrothermal circulation acts to lower oceanic $^{87}Sr/^{86}Sr$ values without changing the concentration, while the carbonate limestone system acts as a buffer for large $^{87}Sr/^{86}Sr$ changes [Elderfield, 1986]. Marine $^{87}Sr/^{86}Sr$ ratios are uniform at any time [e.g., DePaolo and Ingram, 1986] because the residence time of Sr is very long (~2.5-4 m.y.) relative to the mixing time of the oceans (~1000 years)[Broecker and Peng, 1982; Hodell et al., 1990a]. The actual causes of changing $^{87}Sr/^{86}Sr$ through time are not well known. Possible causal mechanisms include changes in (1) continental weathering, which will vary either riverine flux or the $^{87}Sr/^{86}Sr$ ratio of riverine input; (2) hydrothermal flux; or (3) carbonate recycling [Elderfield, 1986].

The nature of observed $^{87}Sr/^{86}Sr$ fluctuations places constraints on the plausible causal mechanisms. Hess et al. [1989] suggest that the cause of $^{87}Sr/^{86}Sr$ fluctuations had time constants of millions of years because the Oligocene-early Miocene $^{87}Sr/^{86}Sr$ increase was apparently linear and monotonic. They therefore attributed Oligocene Sr isotope changes to long-term changes in tectonics which changed riverine flux, $^{87}Sr/^{86}Sr$ of riverine input, or seafloor spreading rates. Both Hess et al. [1989] and Hodell et al. [1989] assumed that variations in seawater $^{87}Sr/^{86}Sr$ may have been proportional to seafloor spreading rates, although Owens and Rea [1985] suggested that changes in hydrothermal flux were not related to spreading rates but to tectonic reorganizations. Based on the apparently monotonic nature of the Oligocene $^{87}Sr/^{86}Sr$ record compared to the transient changes in Oligocene climate, Hess et al. [1989] suggested that climate changes could not readily explain the apparently monotonic $^{87}Sr/^{86}Sr$ changes.

Hodell et al. [1989, 1990a] used models to evaluate possible causes of late Neogene changes in $^{87}Sr/^{86}Sr$. Their models establish that the latest Miocene $^{87}Sr/^{86}Sr$ increase of 0.000100 could be best explained either by an increase in riverine flux or by an increase in the $^{87}Sr/^{86}Sr$ ratio of riverine input through weathering of more sialic crust. Raymo et al. [1988] and Hodell et al. [1989, 1990a] cite evidence for increased riverine flux as a cause of increasing $^{87}Sr/^{86}Sr$ ratios during the late Neogene and ascribed increased flux to uplift and tectonism.

Modeling results also suggest that higher frequency changes could account for large, apparently monotonic changes which occurred on the m.y. scale. The late Miocene $^{87}Sr/^{86}Sr$ increase of 0.000100 occurred within a ~1-m.y. interval, yielding a rate of 0.000100/m.y. [Hodell et al., 1989]. We observe that the early Miocene $^{87}Sr/^{86}Sr$ increase occurred with a rate of 0.000059/m.y. and the Oligocene with a rate of 0.000030/m.y. Hodell et al. [1989] demonstrated that since the residence time of Sr is long and the response of the oceans logarithmic, such large, long-duration increases cannot be explained by simple one-time transfers among reservoirs resulting in a new steady state. However, they demonstrated that such changes potentially can be explained by pulse-like changes in input (figure 3 of Hodell et al. [1989]). These pulse-like changes can readily yield what appear to be monotonic changes such as those on Figure 5.

We suggest the following scenario for Sr isotope changes. This scenario is speculative, but it provides a reasonable reconciliation of the climatic record of Antarctica with the $^{87}Sr/^{86}Sr$ record.

We speculate that the late Eocene-early middle Miocene $^{87}Sr/^{86}Sr$ increases can be explained by intermittent glaciations and deglaciations of the Antarctic continent. We suggest that Oligocene-early Miocene glaciations were intermittent, alternately covering and exposing the east Antarctic craton. As a result, each glaciation caused increases in the flux of sialic weathering products and the mean steady state, which cumulatively resulted in the apparent monotonic (but actually logarithmic) $^{87}Sr/^{86}Sr$ increases (Figure 5).

Antarctic glaciations are expressed in the foraminiferal $\delta^{18}O$ record. Using oxygen isotopes, we previously suggested that there were at least three pulses of Oligocene glaciations at 35.8 Ma, 32.2 Ma, and 28.0 Ma and pulses of early Miocene glaciation at 23.5 Ma, 21.3 Ma, 18.1 Ma, and 16.1 Ma (Figure 5)[Miller et al., 1990a; Wright and Miller, 1990]. There is a physical record of glaciations that suggests that east Antarctica was the site of these glaciations [e.g., Wise et al., 1989; see summary in Miller et al. [1990a]. Thus, the evidence is strong for three Oligocene and four to five early-earliest middle Miocene oxygen isotope increases and associated glaciations (Figure 5).

The timing of the first Cenozoic ice growth event is uncertain. We have argued for the presence of Oligocene ice sheets [Miller and Fairbanks, 1985; Miller et al., 1987, 1990a], but noted that the evidence for middle-late Eocene ice sheets is equivocal. Barron et al. [1989] suggested that the glacial record of Antarctica may have begun in the middle or late Eocene, and we indicated a possible ice growth event for ca. 41 Ma on Figure 5. By assuming that a major late middle Eocene (ca. 42-40 Ma) $\delta^{18}O$ increase [e.g., Kennett and Stott, 1990; Katz and Miller, 1990] is in fact a glacial event, we can reconcile the $\delta^{18}O$ and $^{87}Sr/^{86}Sr$ records (Figure 5).

The overall late Eocene to Oligocene Sr isotope increase of 0.00500 can be explained by four changes in the steady state of ~0.00125 at ca. 41 Ma, 36 Ma, 32 Ma, and 28 Ma. Since the residence time of strontium is 4 m.y. [Broecker and Peng, 1982], each increase would result in a logarithmic change in oceanic mean state of $^{87}Sr/^{86}Sr$ with a half-life concentration attained 2.7 m.y. after each perturbation. (Hodell et al. [1990a] suggested that the residence time of Sr-isotopes in the ocean is closer to 2.5 m.y.; if this is true, half-life concentrations would be obtained after 1.7 m.y.) Assuming a residence time of 4 m.y., a change in the steady state from 0.707650 at ca. 41 to 0.0707800 at ca. 40 Ma (i.e., during the timing of our inferred glaciation) would be observed as an exponential change with the value at 37.3 Ma of 0.0707725. This change would appear to be monotonic at the present resolution (±0.000030). Subsequent changes in the mean state of ~0.000125 due to glaciations at 35.8 Ma, 32.2 Ma, and 28.0 Ma could explain the apparent linear (but actually logarithmic) late Eocene to late Oligocene increase of ~0.00030/m.y.

The increase in the frequency of glaciations during the early Miocene can explain the higher rate of change of $^{87}Sr/^{86}Sr$ at this time. There were four to five periods of inferred glaciation in an 8 m.y. period of the early Miocene (Figure 5)[Wright and

Miller, 1990] versus four late middle Eocene to Oligocene periods of glaciation in a 16-m.y. period (Figure 5). The $^{87}Sr/^{86}Sr$ change of 0.000060/m.y. can be explained by four to five increments in the mean state of ~0.00125-0.00150 due to increased input of sialic glacial weathering products.

There were at least five late middle to early late Miocene glaciations (at 13.6 Ma, 12.6 Ma, 11.3 Ma, 9.6 Ma, and 8.5 Ma [Wright and Miller, 1990]), yet the rate of change of $^{87}Sr/^{86}Sr$ was much lower during this interval (Figure 5). We speculate that by the middle Miocene, a permanent ice cap had developed in east Antarctica [e.g., Shackleton and Kennett, 1975; Savin et al., 1975]. As a result, subsequent glaciations increased the volume, but not the area, of the east Antarctic ice cap and therefore did not significantly change the amount of sialic weathering products.

A large latest Miocene-earliest Pliocene $^{87}Sr/^{86}Sr$ increase (ca. 5.5-4.5 Ma) has been explained as partly reflecting increased glaciation in Antarctica [Hodell et al., 1989]. Similarly, there was apparently a moderate increase in $^{87}Sr/^{86}Sr$ from the "mid-"Pliocene to present which may reflect the high-frequency growth and decay of the northern hemisphere ice sheets [Capo and DePaolo, 1990]. However, Hodell et al. [1990a] suggested that glaciation only accounts for 25% of the Sr isotope increase, and followed Raymo et al. [1988] in ascribing the bulk of the $^{87}Sr/^{86}Sr$ increase due to mountain uplift. Uplift of mountains has played an important role in changing oceanic $^{87}Sr/^{86}Sr$ composition, particularly in the late Neogene [Raymo et al., 1988; Hodell et al., 1989, 1990a,b]. However, it is difficult to specify the timing and magnitude of orogenies, and to separate their effects from changes in climate [Ruddiman et al., 1988; Molnar and England, 1990]. Our empirical linkage of inferred glaciations with late Eocene-Miocene $^{87}Sr/^{86}Sr$ variations is reasonable, although orogenic changes in $^{87}Sr/^{86}Sr$ flux or composition may have played an important role.

CONCLUSION

We developed an isotope reference section for the lower Miocene to lower upper Miocene (~25-8 Ma) by directly tying isotope records ($^{87}Sr/^{86}Sr$, $\delta^{18}O$) into the best available magnetostratigraphic record, DSDP Site 608. This standard provides a time rock calibration for isotope records that is not possible in the shallow water Miocene unit stratotypes.

The Sr isotope record at Site 608 had a high rate of change during the latest Oligocene to early Miocene (ca. 25.1-14.6 Ma) which we approximate with a linear regression (slope = 0.000059/m.y.). Considering our ability to reproduce $^{87}Sr/^{86}Sr$ measurements, Sr isotope stratigraphic resolution may be as good as ±0.5 m.y. for this interval. A lower rate of change occurred from ca. 14.6-8 Ma, and stratigraphic resolution is poor (worse than ±2.3 m.y.).

Calibration of $\delta^{18}O$ records with magnetostratigraphy documents that there were correlatable early to early late Miocene benthic oxygen isotope increases which can be used to define oxygen isotope Zones Mi1, Mi1a, Mi1b, and Mi2-Mi7 [Miller et al., 1990; Wright and Miller, 1990]. These $\delta^{18}O$ increases are global and result partly from increases in ice volume. Recognition of these oxygen isotope zones provides a relatively precise correlation tool with a resolution better than 0.5 m.y.

Comparison of planktonic biostratigraphic ranges against an independent magnetochronology establishes that the ranges of several marker taxa have synchronous first and last occurrences between the subtropics (~30°) and the latitude of Site 608 (43°N). Some taxa exhibit diachronous first or last occurrences. Biostratigraphic resolution is good in the middle Miocene, but poor in the early Miocene; in contrast, Sr isotope resolution is good in the early Miocene but poor in the middle Miocene.

In contrast to Richter and DePaolo [1988], we find that diagenesis is generally a minor problem in shallowly buried (< 400 m) deep-sea sections. We provide a speculative scenario for the causes of the late Eocene-Miocene $^{87}Sr/^{86}Sr$ increase. We attribute a moderate late Eocene-Oligocene $^{87}Sr/^{86}Sr$ increase to four intermittent glaciations of the Antarctic continent in this 14-m.y. interval; these inferred glaciations increased input of sialic glacial weathering products through exposure of the Antarctic craton. The larger early Miocene $^{87}Sr/^{86}Sr$ increase can be attributed to an increased frequency of glacial advances and retreats in east Antarctica. The development of a permanent east Antarctic ice cap during the middle Miocene resulted in a lower rate of increase of $^{87}Sr/^{86}Sr$, since subsequent middle-early late Miocene glaciations increased the volume, but not the areal extent, of the ice sheet.

Acknowledgments. Oxygen isotope studies on Site 608 are part of Ph.D. studies by J.D. Wright. D. Tyler (Rutgers) provided valuable discussions of the statistics. We thank G.D. Jones (Unocal), D.A. Hodell (U. Florida), and R. Koepnick (Mobil) for reviews; R.G. Fairbanks (L-DGO) and D.V. Kent for discussions; and M. E. Katz (L-DGO), C. Troskosky (Rutgers), and J. Zhang (Micropaleo. Press) for technical assistance. This work was supported by National Science Foundation grant OCE87-00005 DDP 89-11810 and Chevron U.S.A. This is Lamont-Doherty Geological Observatory contribution 4695.

REFERENCES

Barron, J.A., et al., *Proceeding Ocean Drilling Program, Initial Reports,* vol. 119, 942 pp., Ocean Drilling Program, College Station, Tex., 1989.

Berggren, W. A., and J. A. VanCouvering, Biochronology, *Stud. Geol., 6,* 39-55, 1974.

Berggren, W. A., and K. G. Miller, Paleogene planktonic foraminiferal biostratigraphy and magnetobiochronology, *Micropaleontology, 34,* 362-380, 1988.

Berggren, W. A., M. P. Aubry, and N. Hamilton, Neogene magnetobiostratigraphy of Deep Sea Drilling Project Site 516 (Rio Grande Rise, South Atlantic), Deep Sea Drilling Project Leg 72, *Initial Rep. Deep Sea Drill. Proj., 72,* 675-713, 1983a.

Berggren, W. A., N. Hamilton, D. A. Johnson, C. Pujol, W. Weiss, P. Cepek, and A. M. Gombos, Jr., Magnetobiostratigraphy of Deep Sea Drilling Project Leg 72, Sites 515–518, Rio Grande Rise (South Atlantic), *Initial Rep. Deep Sea Drill. Proj., 72,* 939-948, 1983b.

Berggren, W. A., D. V. Kent, and J. J. Flynn, Neogene geochronology and chronostratigraphy, *Mem. Geol. Soc. London, 10,* 211-259, 1985.

Blow, W., Late middle Eocene to Recent planktonic foraminiferal biostratigraphy, in *Proceedings of the 1st International Conference on Planktonic Microfossils (Geneva 1967),* vol. 1, pp. 199-422, E.J> Brill, Leiden, 1969.

Blow, W. H., *The Cainozoic Globigerinida,* 1413 pp., E.J. Brill, Leiden, 1979.

Bolli, H. M., Planktonic foraminifera from the Oligocene-Miocene Cipero and Lengua Formations of Trinidad, B.W.I, *Bull. U.S. Nat. Mus., 215,* 97-123, 1957.

Bolli, H. M., and J. B. Saunders, Oligocene to Holocene low latitude planktic foraminifera, in *Plankton Stratigraphy,* edited by H. M. Bolli, J. B. Saunders, and K. Perch-Nielsen, pp. 155-262, Cambridge University Press, New York, 1985.

Bolli, H. M., J. B. Saunders, and K. Perch-Nielsen, (Eds.), *Plankton Stratigraphy,* Cambridge University Press, Cambridge, 1032 pp., Cambridge University Press, New York, 1985.

Broecker, W. S., and T.-H. Peng, *Tracers in the Sea,* 690 pp., Eldigio Press, Palisades, N.Y., 1982.

Burke, W. H., R. E. Denison, E. A. Hetherington, R. B. Koepnick, H. F. Nelson, and J. B. Otto, Variation of seawater $^{87}Sr/^{86}Sr$ throughout Phanerozoic time, *Geology, 10,* 516-519, 1982.

Capo, R.C., and D.J. DePaolo, Seawater Strontium isotopic variations from 2.5 million years ago to the Present, *Science, 249,* 51-55, 1990.

Clement, B., and F. Robinson, The magnetostratigraphy of Leg 94 sediments, *Initial Rep. Deep Sea Drill. Proj., 94,* 635-650, 1986.

Corliss, B.H., M.-P. Aubry, W.A. Berggren, J.M. Fenner, L.D. Keigwin, and G. Keller, The Eocene/Oligocene boundary event in the deep sea, *Science, 226,* 806-810, 1984.

Cowie, J. W., Guidelines for boundary stratotypes, *Episodes, 9,* 78-82, 1986.

Cowie, J. W., W. Zeigler, and J. Remane, Stratigraphic Commission accelerates progress, 1984 to 1989, *Episodes, 12,* 79-83, 1989.

DePaolo, D. J., Detailed record of the Neogene Sr isotopic evolution of seawater from DSDP Site 590B, *Geology, 14,* 103-106, 1986.

DePaolo, D. J., and B. L. Ingram, High-resolution stratigraphy with strontium isotopes, *Science, 227,* 938-940, 1985.

Dowsett, H.J., Diachrony of late Neogene microfossils in the southwest Pacific Ocean: Application of the graphic correlation technique, *Paleoceanography, 3,* 209-222, 1988.

Draper N.R., and H. Smith, Applied Regression Analysis, 709 pp., John Wiley, New York, 1981.

Elderfield, H., Strontium isotope stratigraphy, *Palaeogeogr. Palaeoeclimatol. Palaeoecol., 57,* 71-90, 1986.

Graham, D. W., M. L. Bender, D. F. Williams, and L. D. Keigwin, Sr Ca rations in Cenozoic planktonic foraminifera, *Geochem Cosmochem. Acta, 46,* 1281-1292, 1982.

Haq, B. U., et al., Late Miocene marine carbon isotope shift and synchroneity of some phytoplanktonic biostratigraphic events, *Geology, 8,* 427-431, 1980.

Haq, B. U., J. Hardenbol, and P. R. Vail, Chronology of fluctuating sea levels since the Triassic (250 million years ago to present), *Science, 235,* 1156-1167, 1987.

Hart, S. R., and C. Brooks, Clinopyroxene-matrix partitioning of K, Rb, Cs, and Ba, *Geochim. Cosmochim. Acta, 38,* 1799-1806, 1974.

Hedberg, H., (Ed.), *International Stratigraphic Guide,* 200 pp., John Wiley, New York, 1976.

Hess, J., M. L. Bender, and J.-G. Schilling, Evolution of the ratio of strontium-87 to strontium-86 in seawater from Cretaceous to Present, *Science, 231,* 979-984, 1986.

Hess, J., L.D. Stott, M. L. Bender, J. P. Kennett, and J.-G. Schilling, The Oligocene marine microfossil record: Age assessments using strontium isotopes, *Paleoceanography, 4,* 655-679, 1989.

Hodell, D. A, P. A. Mueller, J. A. McKenzie, and G. A. Mead, Strontium isotope stratigraphy and geochemistry of the late Neogene ocean (9 to 2 Ma), *Earth Planet. Sci. Lett., 92,* 165-178, 1989.

Hodell, D. A, G. A. Mead, and P. A. Mueller, Variation in the strontium isotopic composition of seawater (8 Ma to Present): Implications for chemical weathering rates and dissolved fluxes to the oceans, *Chem. Geol., 80,* in press, 1990a.

Hodell, D. A, P. A. Muller, and J. R. Garrido, Variations in the strontium isotope composition of seawater during the Neogene, *Geology,* in press, 1990b.

Imbrie, J., et al., The orbital theory of Pleistocene climate: Support from a revised chronology of the marine $\delta^{18}O$ record, in *Milankovitch and Climate, Part I,* edited by A. L. Berger, J. Imbrie, J. Hays, G. Kukla, B. Saltzman, pp. 269-305, D. Reidel, Hingham, Mass., 1984.

Jenkins, D.G., Southern mid-latitude Paleocene to Holocene planktonic foraminifera, in *Plankton Stratigraphy,* edited by H. M. Bolli, J. B. Saunders, and K. Perch-Nielsen, pp. 263-282, Cambridge University Press, New York, 1985.

Joyce, J.E., L.R.C. Tjalsma, and J.M. Prutzman, High-resolution planktic stable isotope record and spectral analysis for the last 5.35 m.y.: Ocean Drilling Project site 625 northeast Gulf of Mexico, *Paleoceanography, 5,* 507-529, 1990.

Katz, M. E. , and K. G. Miller, Early Paleogene benthic foraminiferal assemblage and stable isotope composition in the southern ocean, Ocean Drilling Program leg 114, *Proc. Ocean Drilling Prog., 114, Part B,* in press, 1990.

Keigwin, L.D., Paleoceanographic change in the Pacific at the Eocene-Oligocene boundary, *Nature, 287,* 722-725, 1980.

Keigwin, L. D., M.-P. Aubry, and D. V. Kent, North Atlantic late Miocene stable-isotope stratigraphy, biostratigraphy, and magnetostratigraphy, *Initial Rep. Deep Sea Drill. Proj., Part 2,* 935-963, 1986.

Kennett, J. P., Cenozoic evolution of Antarctic glaciation, the circum-Antarctic Ocean, and their impact on global paleoceanography, *J. Geophys. Res., 82,* 3843-3860, 1977.

Kennett, J. P., (Ed.), The Miocene ocean: Paleoceanography and biogeography, *Mem. Geol Soc. Am., 163,* 337 pp., 1985.

Kennett, J. P., and S. Srinivasan, *Neogene Planktonic Foraminifera,* Hutchinson Ross, Stroudsberg, Pa., 265 pp., 1983.

Kennett, J. P., and L. D. Stott, Proteus and Proto-Oceanus: Paleogene oceans as revealed from Antarctic stable isotopic results, *Proc. Ocean Drill. Program, Sci. Results, 113, Part B,* in press, 1990.

Killingley, J. S., Effects of diagenetic recrystallization of $^{18}O/^{16}O$ values of deep-sea sediments, *Nature, 301,* 594-597, 1983.

Koepnick, R. B., W. H. Burke, R. E. Denison, E. A. Hetherington, H. F. Nelson, J. B. Otto, and L.E. Waite, Construction of the seawater $^{87}Sr/^{86}Sr$ curve for the Cenozoic and Cretaceous: Supporting data, Chem. Geol., *58,* 55-81, 1985.

Koepnick, R. B., R. E. Denison, and D. A. Dahl, The Cenozoic seawater $^{87}Sr/^{86}Sr$ curve: Data review and implications for correlations of marine strata, *Paleoceanography, 3,* 743-756, 1988.

Lowrie, W., W. Alvarez, G. Napoleone, K. Perch-Nielson, I. Premoli-Silva, and M. Toumarkine, Paleogene magnetic stratigraphy in Umbrian pelagic carbonate rocks: The

Contessa sections, Gubbio, *Geol. Soc. Am. Bull., 93,* 414-432, 1982.

Ludwig, K. R., R. B. Halley, K. R. Simmons, and Z.E. Peterman, Strontium-isotope stratigraphy of Enewetak Atoll, *Geology, 16,* 173-177, 1988.

Martini, E., Standard Tertiary and Quaternary calcareous nannoplankton zonation, in *Proceedings II Planktonic Conference, Roma, 1970,* vol. 2, edited by A. Farinacci, pp. 739-785, Ediz, Tecnoscienza, Roma, 1971.

McDougall, I., L. Kristjansson, K. Saemundsson, Magnetostratigraphy and geochronology of northwest Iceland, *J. Geophys. Res., 89,* 7029-7060, 1984.

McKenzie, J. A., D. A. Hodell, P.A. Mueller, and D. W. Muller, Application of strontium isotopes to late Miocene-early Pliocene stratigraphy, *Geology, 16,* 1022-1025, 1988.

McNeil, D. H., and K. G. Miller, Sr isotope and benthic foraminiferal correlations of Arctic strata (Nuwok Beds, Alaskan North Slope) to standard Oligocene chronostratigraphy, *Geology, 18,* 415-418, 1990

Miller, K. G., and R. G. Fairbanks, Oligocene-Miocene global carbon and abyssal circulation changes, in *The Carbon Cycle and Atmospheric CO_2: Natural Variations Archean to Present, Geophys. Monogr. Ser.,* vol. 32, edited by E. Sundquist, and W. S. Broecker, pp. 469-486, AGU, Washington, D. C., 1985.

Miller, K. G., and D. V. Kent, Testing Cenozoic eustatic changes: The critical role of stratigraphic resolution, *Spec. Publ. Cushman Found. Foraminiferal Res., 24,* 51-56, 1987.

Miller, K. G., M. P. Aubry, M. J. Khan, A. J. Melillo, D. V. Kent, and W. A. Berggren, Oligocene to Miocene biostratigraphy, magnetostratigraphy, and isotopic stratigraphy of the western North Atlantic, *Geology, 13,* 257-261, 1985.

Miller, K. G., R. G. Fairbanks, and E. Thomas, Benthic foraminiferal carbon isotope records and the development of abyssal circulation in the eastern North Atlantic, *Initial Rep. Deep Sea Drill. Proj., 94,* 981-996, 1986.

Miller, K.G., R. G. Fairbanks, and G. S. Mountain, Tertiary oxygen isotope synthesis, sea-level history, and continental margin erosion, *Paleoceanography, 2,* 1-19, 1987.

Miller, K.G., M. D. Feigenson, D. V. Kent, and R. K. Olsson, Oligocene stable isotope ($^{87}Sr/^{86}Sr$, $\delta^{18}O$, $\delta^{13}C$) standard section, Deep Sea Drilling Project site 522, *Paleoceanography, 3,* 223-233, 1988.

Miller, K. G., J. D. Wright, and A. N. Brower, Oligocene to middle Miocene stable isotope stratigraphy and planktonic foraminiferal biostratigraphy of the Sierra Leone Rise (Sites 366 and 667), *Proc. Ocean Drill. Program, Sci. Results, 108, Part B,* 279-294, 1989.

Miller, K. G., J. D. Wright, and R. G. Fairbanks, Unlocking the Ice House: Oligocene-Miocene oxygen isotopes, eustasy, and margin erosion, *J. Geophys. Res.,* in press, 1990a.

Miller, K. G., D. V. Kent, A. N. Brower, L. Bybell, M. D. Feigenson, R. K. Olsson, and R. Z. Poore, Eocene-Oligocene sea-level changes on the New Jersey coastal plain linked to the deep-sea record, *Geol. Soc. Am. Bull., 102,* 331-339, 1990b.

Molnar, P., and P. England, Late Cenozoic uplift of mountain ranges and global climate change: Chicken or egg?, *Nature, 346,* 29-34, 1990.

Oberhansli, H., and M. Toumarkine, The Paleogene oxygen and carbon isotope history of sites 522, 523, and 524 from the central South Atlantic, in *South Atlantic Paleoceanography,* edited by K. J. Hsu and H. J. Weissert, pp. 124-147, Oxford University Press, New York, 1985.

Oberhansli, H., J. McKenzie, M. Toumarkine, and H. Weissert, A paleoclimatic and paleoceanographic record of the Paleogene in the central South Atlantic (leg 73) sites 522, 523, and 524), *Initial Rep. Deep Sea Drill. Proj., 78,* 737-747, 1984.

Owens, R. E., and D. K. Rea, Sea-floor hydrothermal activity links climate to tectonics: The Eocene CO_2 greenhouse, *Science, 227,* 166-169, 1985.

Pisias, N. G., N. J. Shackleton, and M. A. Hall, Stable isotope and calcium carbonate records from hydraulic piston cored hole 574A: High-resolution records from the middle Miocene, *Initial Rep. Deep Sea Drill. Proj., 85,* 735-748, 1985.

Poore, R. Z., and R. K. Matthews, Late Eocene-Oligocene oxygen and carbon isotope record from South Atlantic Ocean DSDP site 522, *Initial Rep. Deep Sea Drill. Proj., 73,* 725-736, 1984.

Poore, R. Z., L. Tauxe, S.F. Percival, Jr., J. L. LaBrecque, Late Eocene-Oligocene magnetostratigraphy and biostratigraphy at South Atlantic DSDP site 522, *Geology, 10,* 508-511, 1982.

Premoli-Silva, I., R. Coccioni, and A. Montanari, (Eds.), *The Eocene-Oligocene Boundary in the Marche-Umbria Basin (Italy),* 268 pp., Spec. Publ. International Subcommission Paleogene Stratigraphy, Ancona, Italy, 1988.

Pujol, C., Cenozoic planktonic foraminiferal biostratigraphy of the southwestern Atlantic (Rio Grande Rise): Deep Sea Drilling Project leg 72, *Initial Rep. Deep Sea Drill. Proj., 72,* 623-674, 1983.

Raymo, M., W. F. Ruddiman, and P. N. Froelich, Influence of late Cenozoic mountain building on ocean geochemical cycles, *Geology, 16,* 649-653, 1988.

Raymo, M., W. F. Ruddiman, J. Backman, B. M. Clement, and D. G. Martinson, Late Pliocene variation in northern hemisphere ice sheets and North Atlantic Ocean, *Paleoceanography, 4,* 413-446, 1989.

Richter, F. M., and D. J. DePaolo, Diagenesis and Sr isotopic evolution of seawater using data from DSDP 590B and 575, *Earth Planet. Sci. Lett., 90,* 382-384, 1988.

Ruddiman, W. F., M. Raymo, and A. McIntyre, Matuyama 41,000-year cycles: North Atlantic Ocean and northern hemisphere ice sheets, *Earth Planet. Sci. Lett., 80,* 117-129, 1986a.

Ruddiman, W. F., et al., *Initial Reports Deep Sea Drill. Project,* vol. 94, 1261 pp., U.S. Government Printing Office, Washington, D.C., 1986b.

Ruddiman, W. F., W. L. Prell, and M. Raymo, Late Cenozoic uplift in southern Asia and the American west: Rationale for general circulation modeling experiments, *J. Geophys. Res., 94,* 18,393-18,407, 1988.

Rundberg, Y., and P. C. Smalley, High-resolution dating of Cenozoic sediments from northern North Sea using $^{87}Sr/^{86}Sr$ stratigraphy, *AAPG Bull., 73,* 298-308, 1989.

Savin, S. M., R. G. Douglas, and F. G. Stehli, Tertiary marine paleotemperatures, *Geol. Soc. Am. Bull., 86,* 1499-1510, 1975.

Savin, S.M., G. Keller, R. G. Douglas, J. S. Killingley, L. Shaughnessy, M. A. Sommer, E. Vincent, and F. Woodruff, Miocene benthic foraminiferal isotope records: A synthesis, *Mar. Micropaleontology, 6,* 423-450, 1981.

Shackleton, N. J., and J. P. Kennett, Paleotemperature history of the Cenozoic and initiation of Antarctic glaciation: Oxygen and carbon isotopic analyses in DSDP sites 277,

279, and 281, *Initial Rep. Deep Sea Drill. Proj.*, *29*, 743-755, 1975.

Shackleton, N. J., and N. D. Opdyke, Oxygen isotopic and palaeomagnetic stratigraphy of equatorial Pacific core V28-238: Oxygen isotope temperatures and ice volume on a 10^5 to 10^6 year scale, *Quat. Res.*, *3*, 39-55, 1973.

Takayama, T., and T. Sato, Coccolith biostratigraphy of the North Atlantic Ocean, Deep Sea Drilling Project leg 94, *Initial Report Deep Sea Drill. Proj.*, *94*, 651-702, 1986.

Tauxe, L., P. Tucker, N. P. Petersen, and J. L. LaBrecque, Magnetostratigraphy of leg 73 sediments, *Palaeogeogr. Palaeoclimatol. Palaeoecol.*, *42*, 65-90, 1983.

Tauxe, L., P. Tucker, N. P., Peterson, and J. L. LaBrecque, Magnetostratigraphy of leg 73 sediments, *Initial Rep. Deep Sea Drill. Proj.*, *73*, 609-612, 1984.

Vincent, E., J.S. Killingley, and W.H. Berger, Miocene oxygen and carbon isotope stratigraphy of the tropical Indian Ocean, in The Miocene Ocean: Paleoceanography and Biogeography, edited by J.P. Kennett, *Mem. Geol. Soc. Am.*, *163*, 103-130, 1985.

Weaver, P. P. E., and B. M. Clement, Magnetobiostratigraphy of planktonic foraminiferal datums: Deep Sea Drilling Project leg 94, North Atlantic, *Initial Rep. Deep Sea Drilling Proj.*, *94*, 815-829, 1986.

Wise, S.W., et al., *Proceeding Ocean Drilling Program, Initial Reports*, vol.120, Ocean Drilling Program, College Station, Tex., 1989.

Woodruff, F., S. M. Savin, and R. G. Douglas, Miocene stable isotope record: A detailed deep Pacific Ocean study and its paleoclimatic implications, *Science*, *212*, 665-668, 1981.

Wright, J. D., and K. G. Miller, Miocene stable isotope stratigraphy, site 747, Kerguelen Plateau, *Proc. Ocean Drill. Program*, *120*, *Sci. Results, Part B*, in press, 1990.

Wright, J.D., K.G. Miller, and R.G. Fairbanks, Evolution of modern deep-water circulation: Evidence from the late Miocene southern ocean, *Paleoceanography*, in press, 1990.

York, D., The best isochron, *Earth Planet. Sci. Lett.*, *2*, 479-482, 1967.

B.M. Clement, Department of Geology, Florida International University, Miami FL 33199

M. D. Feigenson and K.G. Miller, Department of Geological Sciences, Rutgers University, New Brunswick, N.J. 08903.

J.D. Wright, Lamont-Doherty Geological Observatory of Columbia University, Palisades, N.Y. 10964.

(Received April 13, 1990;
revised August 28, 1990;
accepted August 29, 1990.)